

Supporting Information for:

**Effect of Modulator Ligands on the
Growth of Co₂(dobdc) Nanorods**

*Nina S. Pappas, Jarad A. Mason**

*email: mason@chemistry.harvard.edu

List of Contents

1. Materials and Methods.....	S-3
2. Synthesis of Co₂(dobdc) nanoparticles.....	S-3
3. Powder X-Ray Diffraction	S-5
4. Thermogravimetric Analysis	S-7
5. Dynamic Light Scattering Analysis.....	S-8
6. Transmission Electron Microscopy.....	S-10
7. BET and External Surface Area.....	S-19
8. CO₂ Adsorption Isotherms.....	S-28
9. Quantification of Bound Modulator.....	S-29
T1 Analysis	S-29
Nuclear Magnetic Resonance Spectroscopy (NMR).....	S-30
External Surface Coverage Model	S-42
Hammett Plot	S-43
10. Modulator pK_a Values	S-44
11. References	S-45

Materials and Methods

Reagents and solvents were purchased from commercial vendors and used as received. Powder X-ray diffraction patterns were measured at ambient temperature using a D2 Phaser Bruker AXS diffractometer with $\text{CuK}\alpha$ radiation ($\lambda = 1.5418 \text{ \AA}$). Thermogravimetric Analysis (TGA) experiments were run on a TGA 550 from TA Instruments in open aluminum pans with a stainless-steel bail under air and heated at a rate of 2–5 °C/min under a 10 mL/min N_2 flow from ambient temperature to 600 °C with an empty aluminum pan/stainless steel bail used as the reference. The TGA mass was calibrated using a series of 3 reference masses, while the TGA temperature was calibrated to the Curie temperature of Ni. DLS measurements were performed using a Malvern Zetasizer Ultra. Transmission electron microscopy (TEM) experiments were performed by dispersing dried $\text{Co}_2(\text{dobdc})$ nanorods in methanol via sonication for 5 min. The solutions were then diluted 10-fold and dropcast on a copper TEM grid. Images were obtained using a HT7800 series TEM operating at an accelerating voltage of 80 kV. Over 100 nanorods were imaged and measured to obtain size distributions for each sample. Langmuir surface area measurements were performed using a Micromeritics 3Flex 3500 instrument. In a typical measurement, 30–100 mg of powder was transferred to a pre-weighed glass measurement tube and capped with a Micromeritics Transeal. The sample was then degassed at 175 °C on a Micromeritics SmartVacPrep equipped with a turbomolecular pump. The evacuated tube was then weighed to determine the mass of the degassed sample. The sample was then fitted with an isothermal jacket and transferred to 3Flex analysis port. Langmuir surface areas were measured in a 77 K liquid N_2 bath and calculated using the Micromeritics software assuming a cross-sectional area of 16.2 \AA^2 for N_2 . ^1H NMR spectra of digested $\text{Co}_2(\text{dobdc})$ nanorods were collected with T_1 values for all species obtained via the inversion-recovery method. Samples were prepared by dispersing ~5 mg of dried $\text{Co}_2(\text{dobdc})$ powder in a solution of 10 μL of 35 wt. % DCl in D_2O and 0.7 mL of DMSO-d_6 . The solution was sonicated until the solid was fully dissolved. ^1H NMR spectra were collected on a Bruker Avance NMR spectrometer at 400MHz. Titration experiments were performed using a Mettler Toledo Seven Excellence pH meter (S400-Micro). In a typical measurement, 30 mg of modulator was dissolved in 1 mL of 1 M NaOH , which was subsequently diluted with 30 mL of water and titrated against a 0.1 M HCl solution.

Synthesis of $\text{Co}_2(\text{dobdc})$ nanoparticles

Synthesis of $\text{Co}_2(\text{dobdc})$ nanorods with 1 equivalent of salicylic acid modulators.

Nanorods were prepared by following a procedure adapted from a previous report.¹ Specifically, $\text{H}_2(\text{dobdc})$ ($\text{H}_2\text{dobdc} = 2,5\text{-dihydroxy-1,4-benzenedicarboxylic acid}$; 99 mg, 0.5 mmol, 1 eq) was combined with a given salicylic acid modulator (0.5 mmol, 1 eq) in a 20-mL vial, then 6.5 mL of a 4:1 (v/v) solution of $\text{DMF} : \text{H}_2\text{O}$ was added. The solution was sonicated until translucent. In a separate 20-mL vial, $\text{Co}(\text{OAc})_2 \cdot 4\text{H}_2\text{O}$ (323 mg, 1.3 mmol, 2.6 eq) was combined with 6.5 mL of a 4:1 (v/v) solution of $\text{DMF} : \text{H}_2\text{O}$ and sonicated until translucent. The Co solution was then added dropwise to the stirring ligand solution, and the resulting solution was quickly transferred to a 15-mL Teflon-lined autoclave and heated in an oven at 130 °C for 24 h. The product was collected

through centrifugation and purified by soaking three times in 40 mL of DMF at room temperature for at least 2 h followed by soaking 10 times in 40 mL of MeOH at room temperature for at least 2 h. The samples were dried in a desiccator prior to additional characterization.

Synthesis of Co₂(dobdc) nanorods with variable equivalents of salicylic acid modulators.

Nanorods were synthesized following the preparation and purification described above with 1.5, 2, or 3 equivalents of modulator used.

Synthesis of Co₂(dobdc) with 1 equivalent of benzoic acid modulators.

Co₂(dobdc) nanoparticles were synthesized following the preparation and purification described above using 1 equivalent of either 4-trifluoromethylbenzoic acid, benzoic acid, or 4-methoxybenzoic acid.

Synthesis of Co₂(dobdc) nanorods with mixed modulators.

Nanorods were synthesized following the preparation and purification described above with 1 equivalent of 4-trifluoromethylsalicylic acid and 1 equivalent of 4-methoxysalicylic acid.

Synthesis of salicylic acid Co₂(dobdc) nanorods with variable reaction time.

Nanorods were synthesized following the preparation described above with 1 equivalent of salicylic acid. Reactions were allowed to heat in the Teflon-lined autoclave for either 1 day, 2 days, or 3 days. Nanorods were then purified following the procedure described above.

Ligand Exchange Reaction.

Nanorods were first synthesized following the procedures described above with salicylic acid as the modulator. After the initial reaction was complete, the Teflon-lined autoclave was opened, and 4-trifluoromethyl salicylic acid was added to the reaction slurry (2 equivalents). The autoclave was re-sealed and returned to the oven at 130 °C for 24 h. The nanorods were then washed and purified following the procedure described above.

Powder X-Ray Diffraction

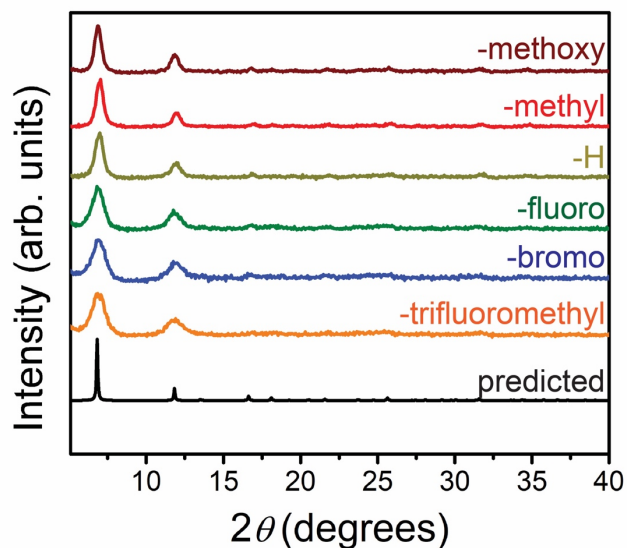


Figure S1. Ambient temperature Powder X-Ray diffraction patterns of Co₂(dobdc) nanorods synthesized with 1 equivalent of various salicylic acid modulators. The black trace corresponds to the predicted diffraction pattern from the Co₂(dobdc) crystal structure.²

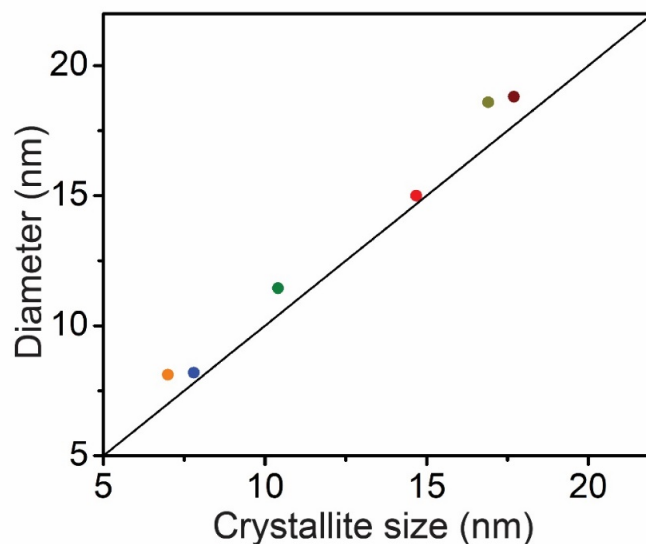


Figure S2. Diameters, as measured by transmission electron microscopy, and crystallite sizes, as calculated by the Scherrer equation, for Co₂(dobdc) nanorods synthesized with 1 equivalent of various salicylic acid modulators. Black line represents a linear relationship with a slope of 1 and is added to guide the eye.

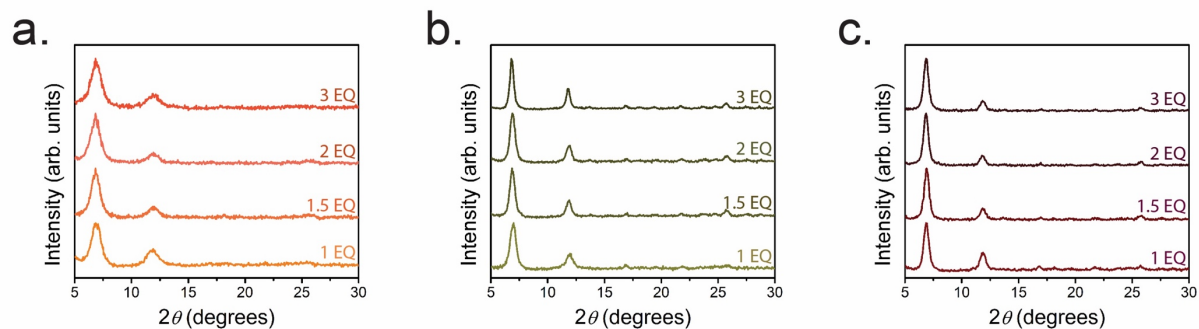


Figure S3. Ambient temperature Powder X-Ray diffraction patterns of $\text{Co}_2(\text{dobdc})$ nanorods synthesized with variable equivalents of (a) 4-trifluoromethylsalicylic acid, (b) salicylic acid, (c) 4-methoxysalicylic acid.

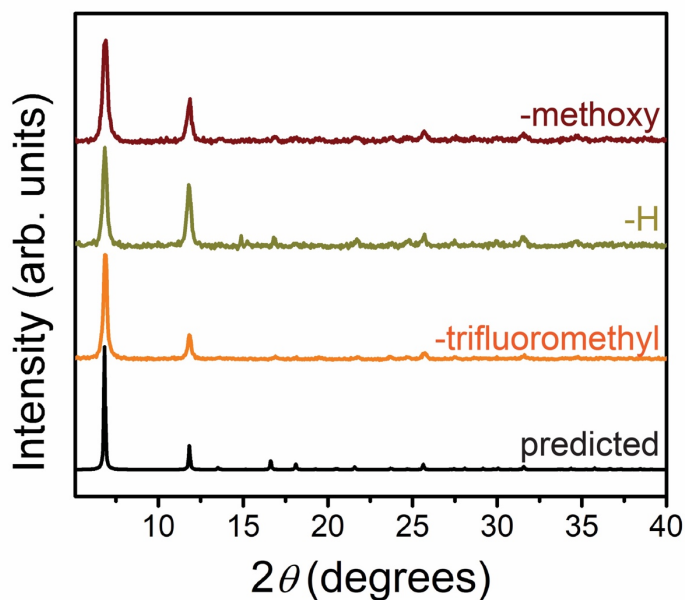


Figure S4. Ambient temperature Powder X-Ray diffraction patterns of $\text{Co}_2(\text{dobdc})$ nanorods synthesized with 1 equivalent of various benzoic acid modulators. The black trace corresponds to the predicted diffraction pattern from the $\text{Co}_2(\text{dobdc})$ crystal structure.²

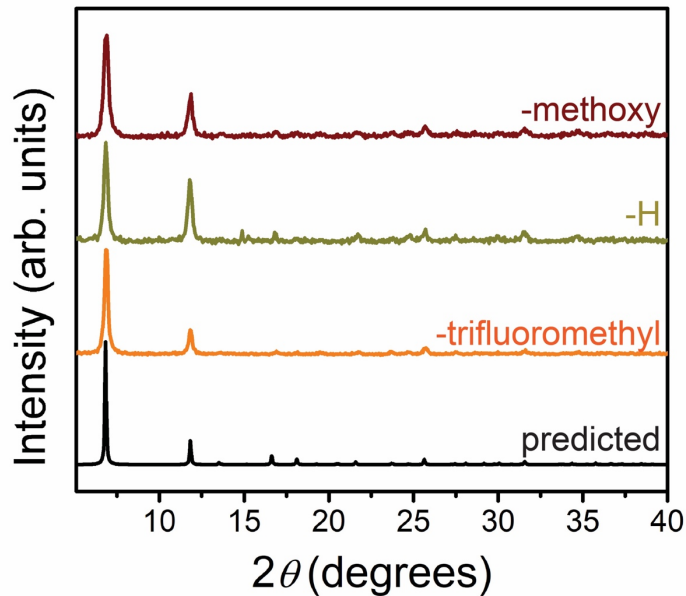


Figure S5. Ambient temperature Powder X-Ray diffraction patterns of $\text{Co}_2(\text{dobdc})$ nanorods surface exchanged with (- CF_3 /-Br). The black trace corresponds to the predicted diffraction pattern from the $\text{Co}_2(\text{dobdc})$ crystal structure.²

Thermogravimetric Analysis

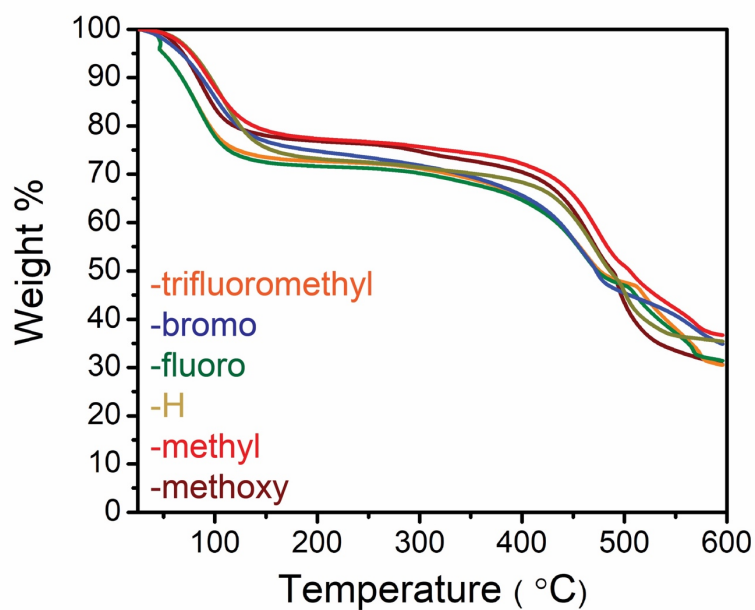


Figure S6. Thermogravimetric analysis (TGA) of $\text{Co}_2(\text{dobdc})$ nanorods synthesized with 1 equivalent of various salicylic acid modulators.

Dynamic Light Scattering Analysis

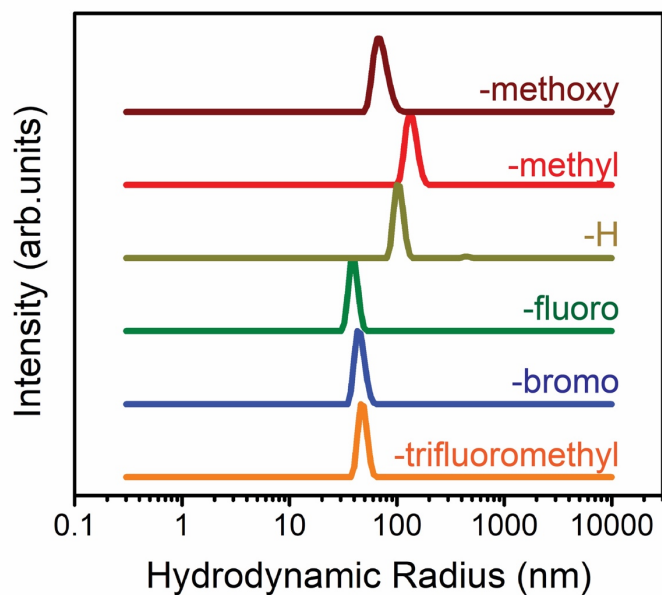


Figure S7. Dynamic light scattering (DLS) measurements of methanolic solutions of $\text{Co}_2(\text{dobdc})$ nanorods synthesized with 1 equivalent of various salicylic acid modulators.

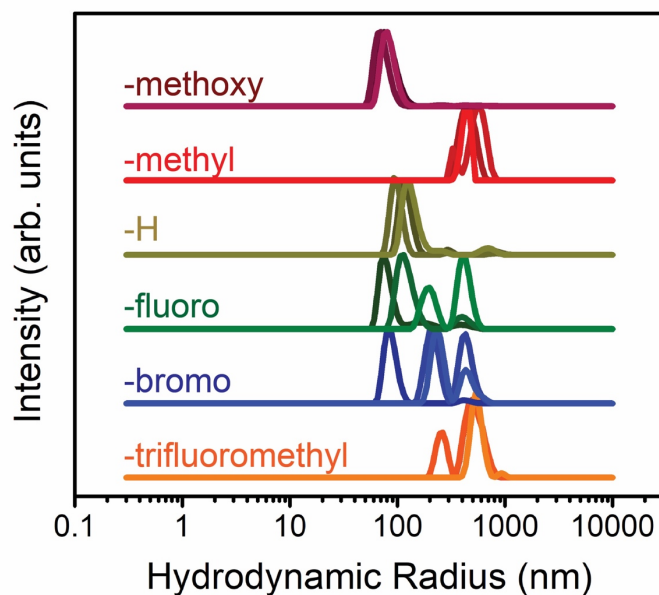


Figure S8. DLS measurements of aqueous solutions of $\text{Co}_2(\text{dobdc})$ nanorods synthesized with 1 equivalent of various salicylic acid modulators. Measurements were collected 3 times with a 6-min delay between consecutive runs.

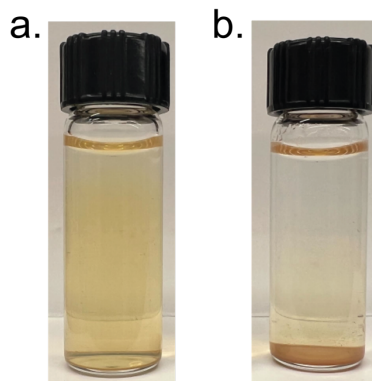


Figure S9. Aqueous solutions (0.5 mg/mL) of $\text{Co}_2(\text{dobdc})$ nanorods synthesized with 1 equivalent (a) 4-methoxysalicylic acid and (b) 4-trifluoromethylsalicylic acid, which highlight the greater aggregation—and lower colloidal stability—observed for 4-trifluoromethylsalicylic acid. Images show solutions after being left undisturbed for 1 week.

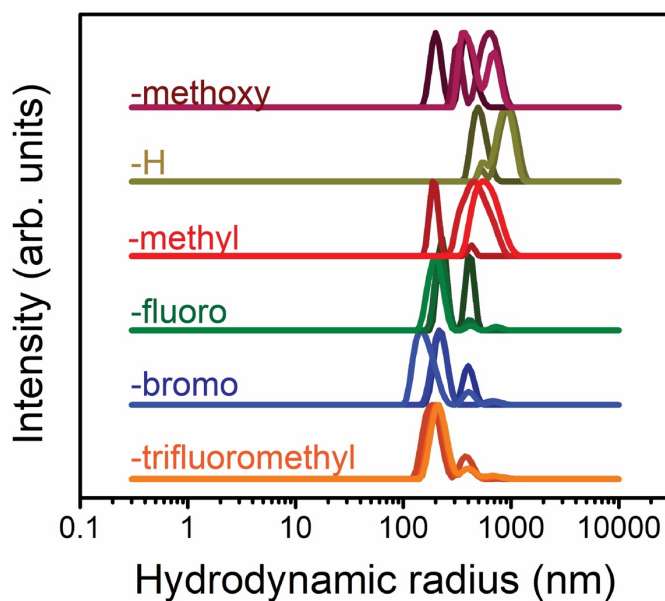


Figure S10. DLS measurements of toluene solutions of $\text{Co}_2(\text{dobdc})$ nanorods synthesized with 1 equivalent of various salicylic acid modulators. Measurements were collected 3 times with a 6-min delay between consecutive runs.

Transmission Electron Microscopy

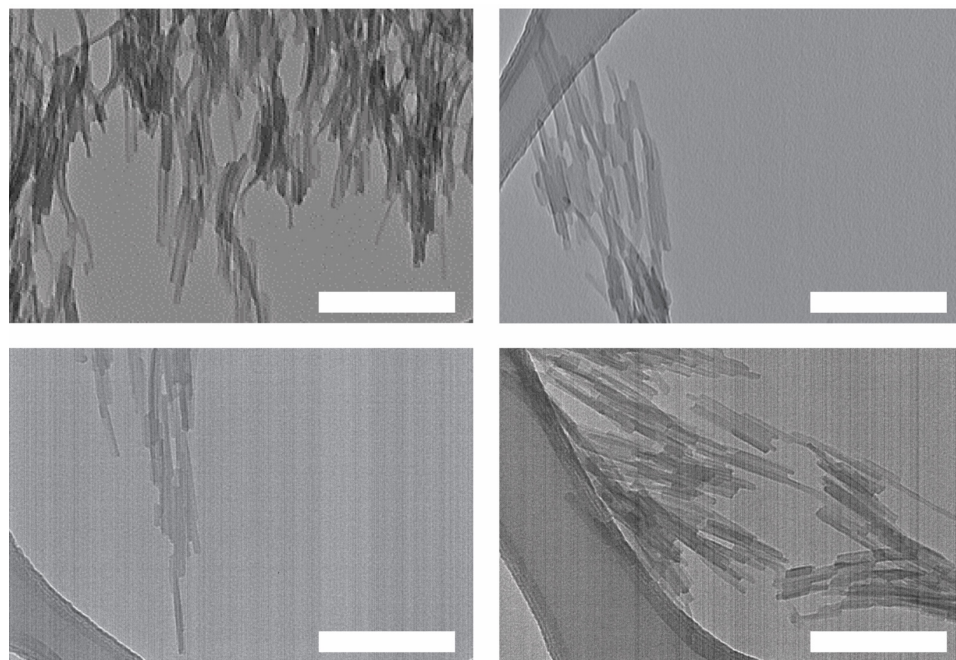


Figure S11. Representative transmission electron microscopy (TEM) images of $\text{Co}_2(\text{dobdc})$ nanorods synthesized with 1 equivalent of 4-trifluoromethylsalicylic acid. Scale bars: 200 nm.

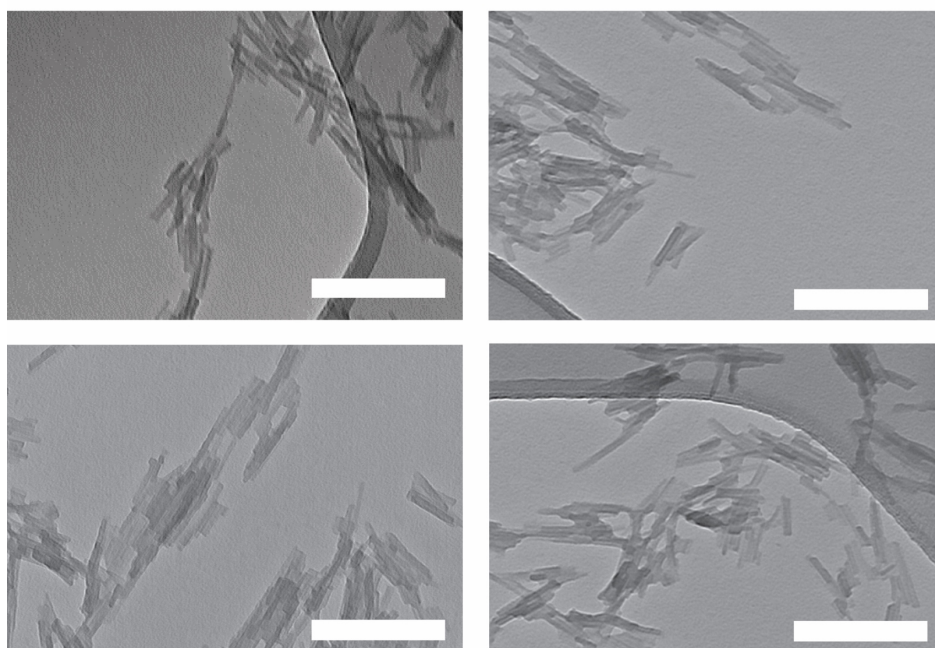


Figure S12. Representative TEM images of $\text{Co}_2(\text{dobdc})$ nanorods synthesized with 1 equivalent of 4-bromosalicylic acid. Scale bars: 200 nm.

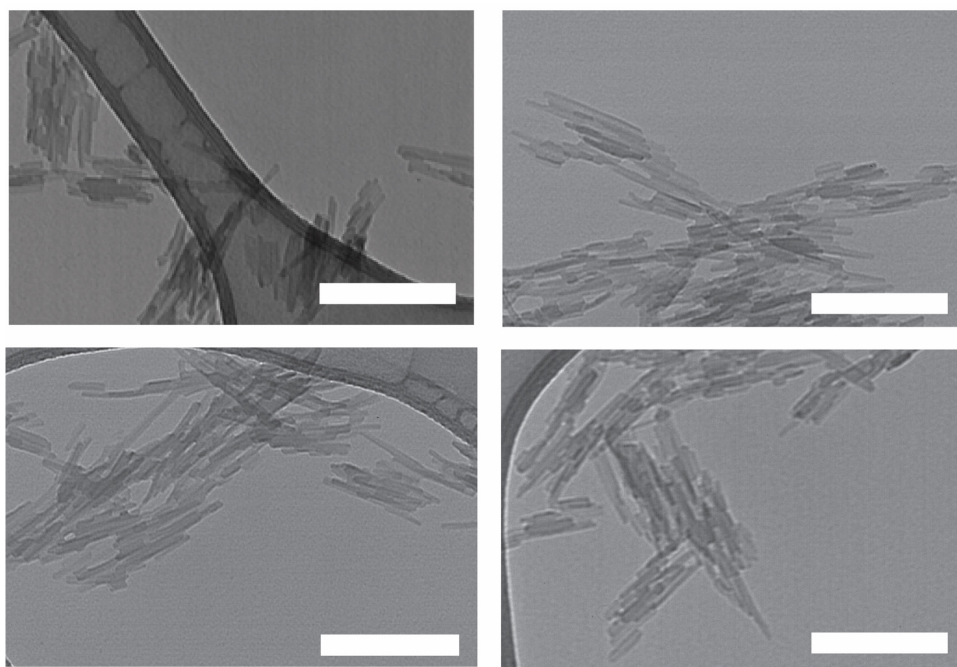


Figure S13. Representative TEM images of $\text{Co}_2(\text{dobdc})$ nanorods synthesized with 1 equivalent of 4-fluorosalicylic acid. Scale bars: 200 nm.

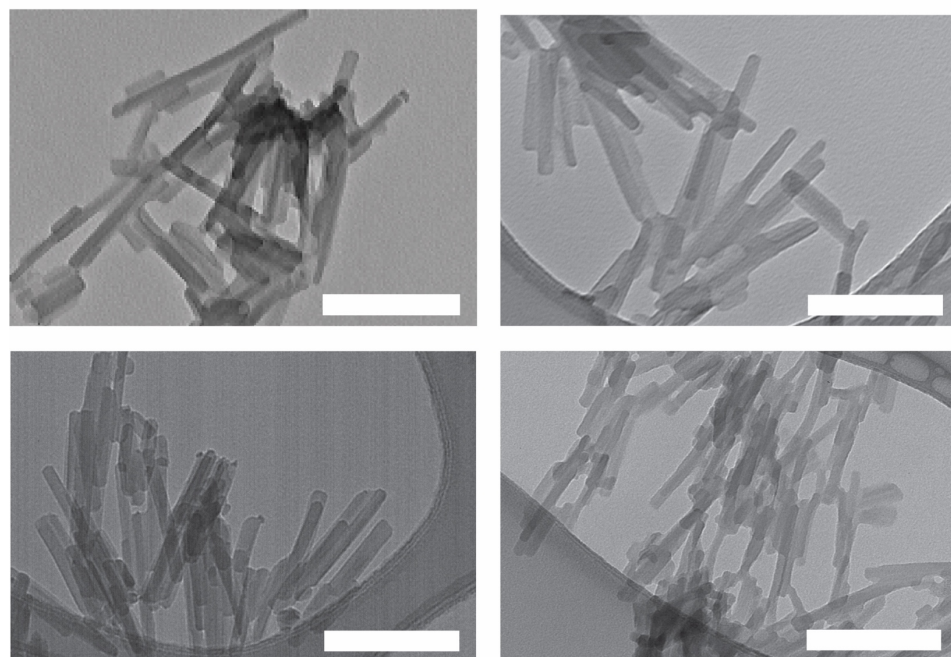


Figure S14. Representative TEM images of $\text{Co}_2(\text{dobdc})$ nanorods synthesized with 1 equivalent of salicylic acid. Scale bars: 200 nm.

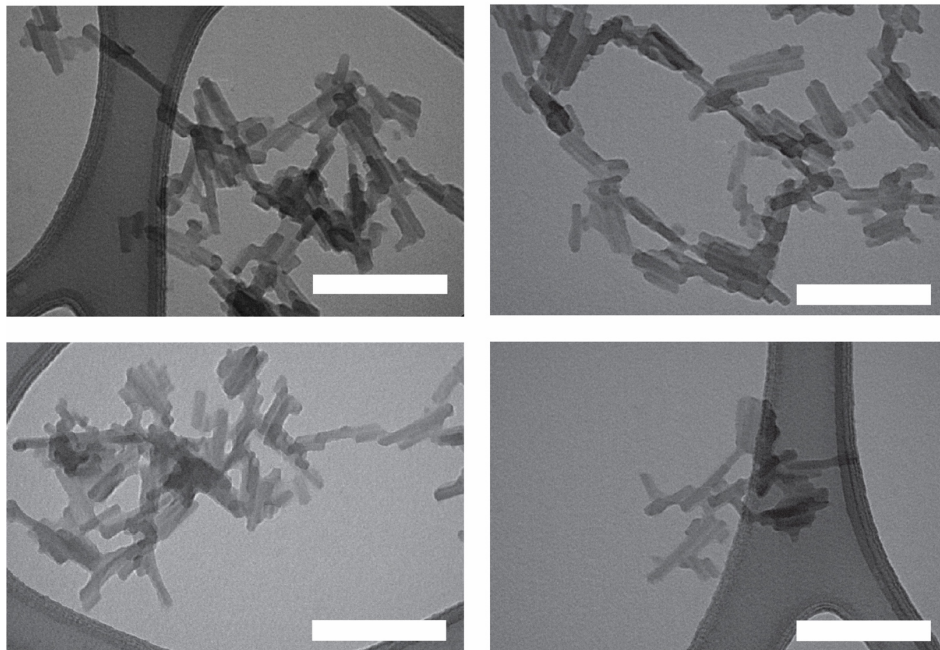


Figure S15. Representative TEM images of $\text{Co}_2(\text{dobdc})$ nanorods synthesized with 1 equivalent of 4-methylsalicylic acid. Scale bars: 200 nm.

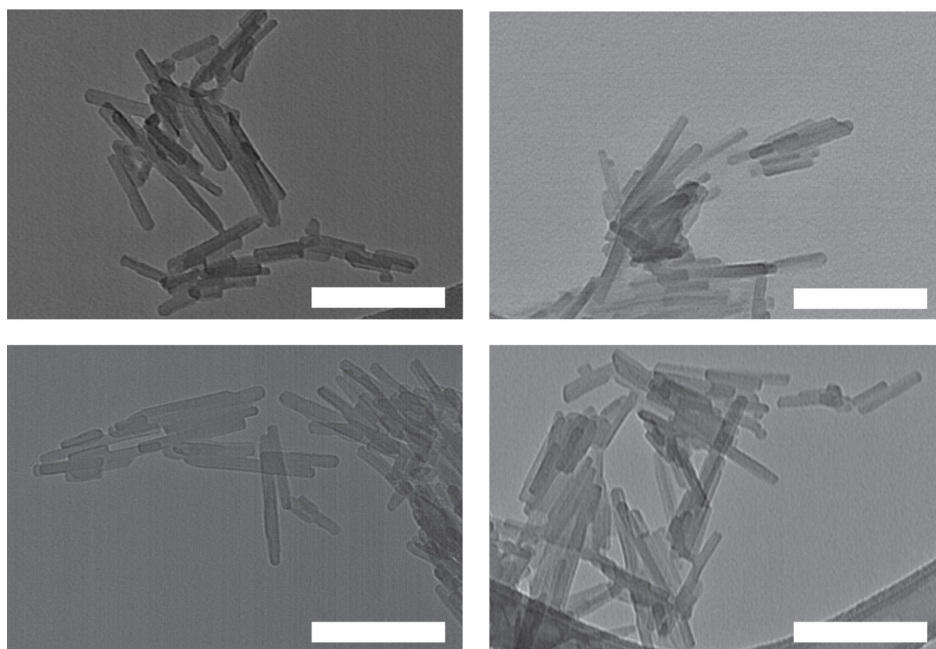


Figure S16. Representative TEM images of $\text{Co}_2(\text{dobdc})$ nanorods synthesized with 1 equivalent of 4-methoxysalicylic acid. Scale bars: 200 nm.

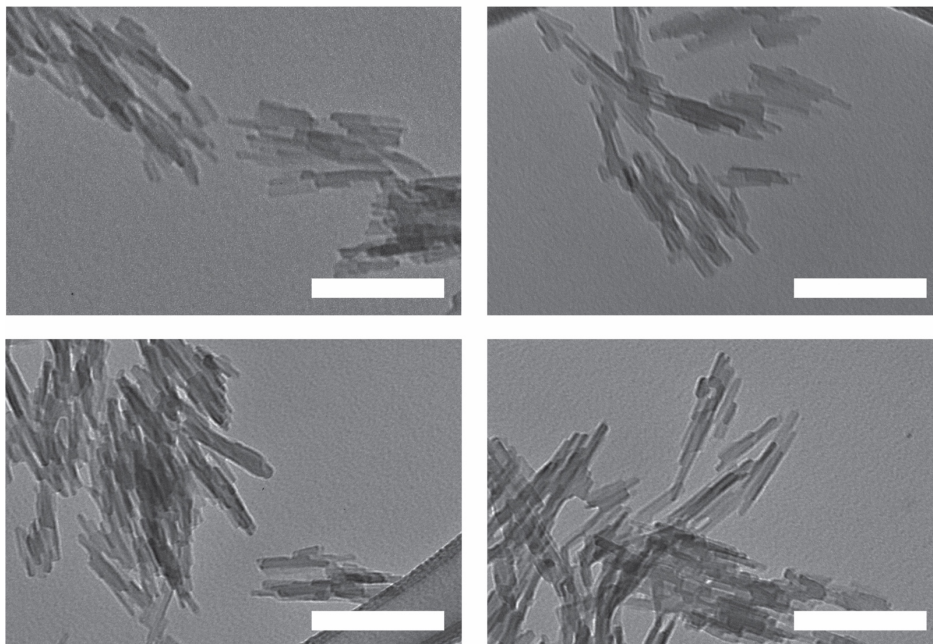


Figure S17. Representative TEM images of $\text{Co}_2(\text{dobdc})$ nanorods synthesized with a mixed modulator system (1 equivalent of 4-methoxysalicylic acid and 1 equivalent of 4-trifluoromethylsalicylic acid). Scale bars: 200 nm.

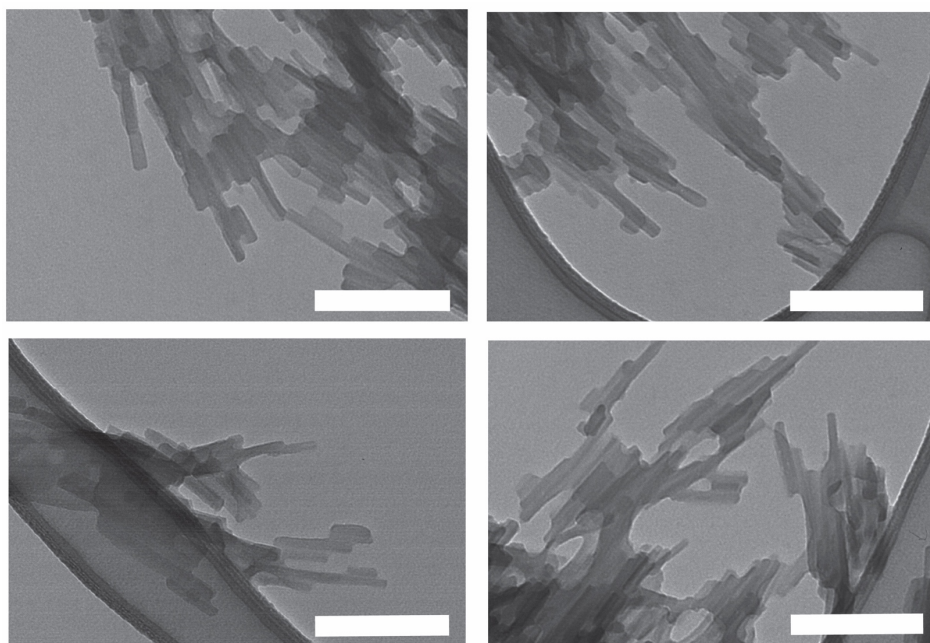


Figure S18. Representative TEM images of surface exchanged $\text{Co}_2(\text{dobdc})$ nanorods synthesized first with salicylic acid and then exchanged with 4-trifluoromethylsalicylic acid. Scale bars: 200 nm.

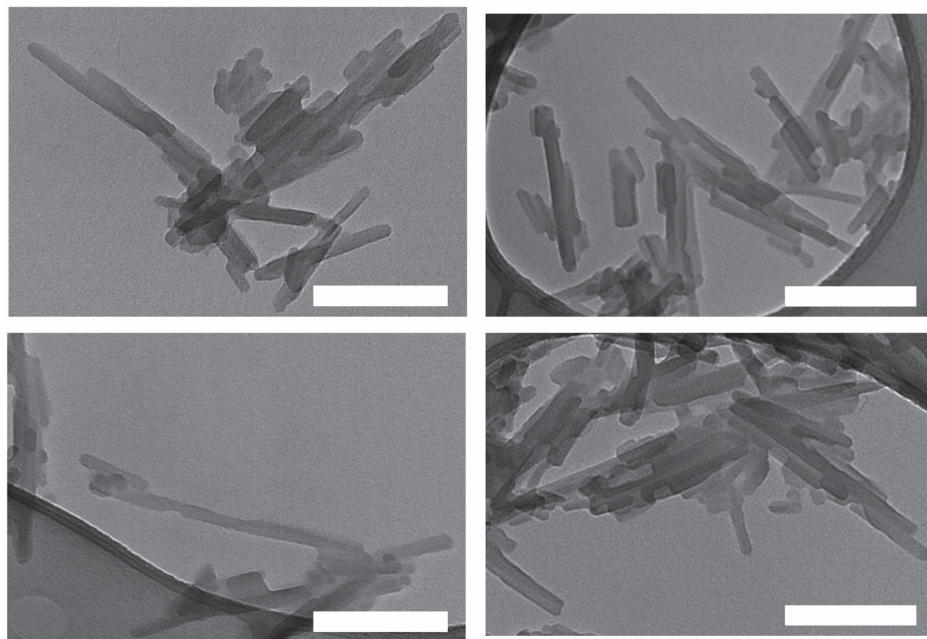


Figure S19. Representative TEM images of Co₂(dobdc) nanorods synthesized with salicylic acid with a reaction time of 2 days. Scale bars: 200 nm.

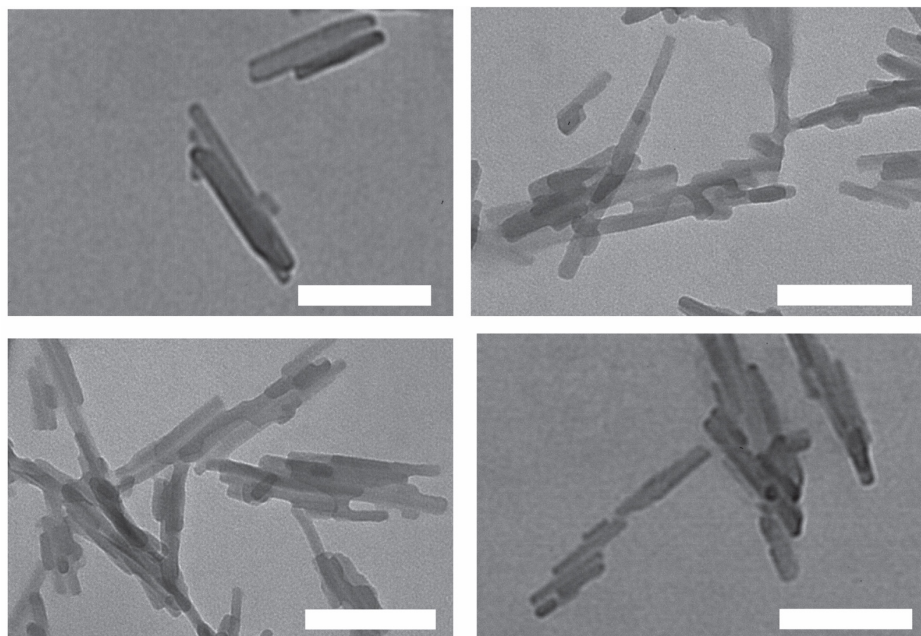


Figure S20. Representative TEM images of Co₂(dobdc) nanorods synthesized with salicylic acid with a reaction time of 3 days. Scale bars: 200 nm.

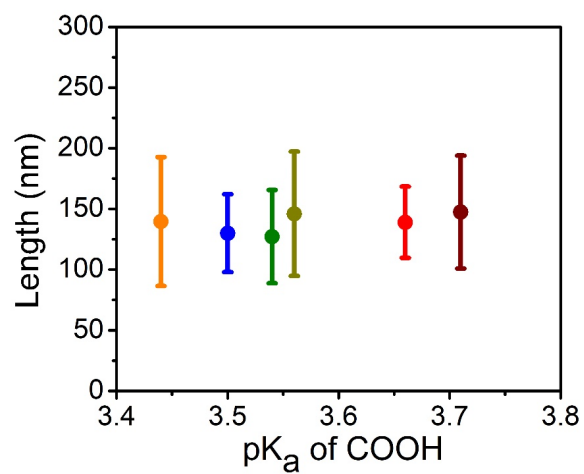


Figure S21. Nanorod lengths, as measured by TEM, for Co₂(dobdc) nanorods synthesized with 1 equivalent of various salicylic acid modulators.

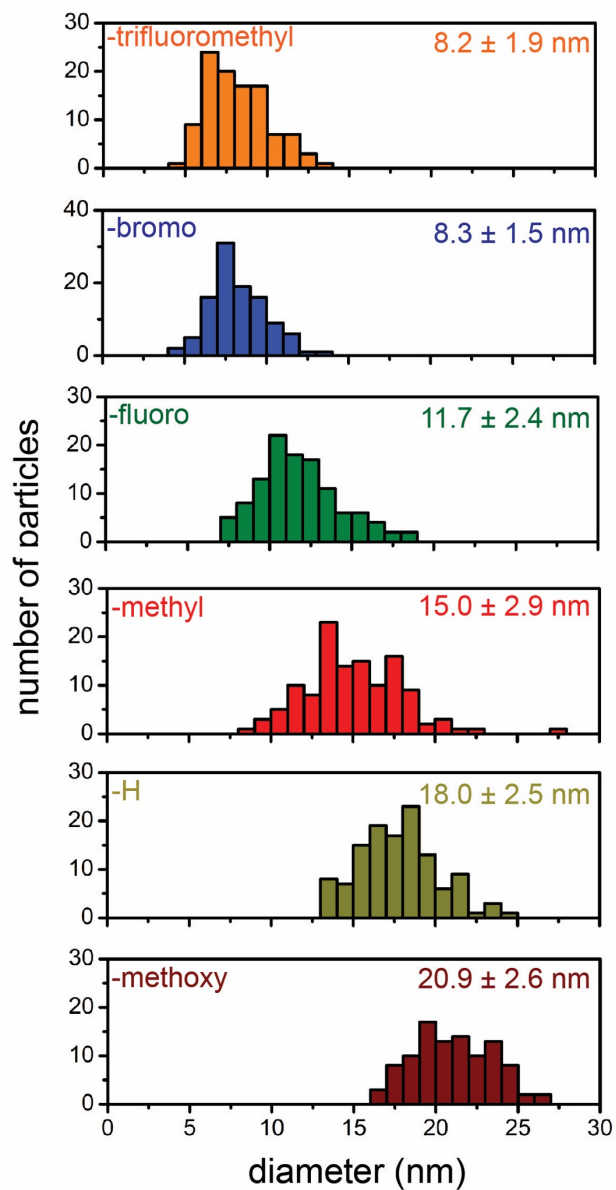


Figure S22. Nanorod size distributions for syntheses conducted with 1 equivalent of salicylic acid-based modulator as determined from representative TEM images of at least 100 particles.

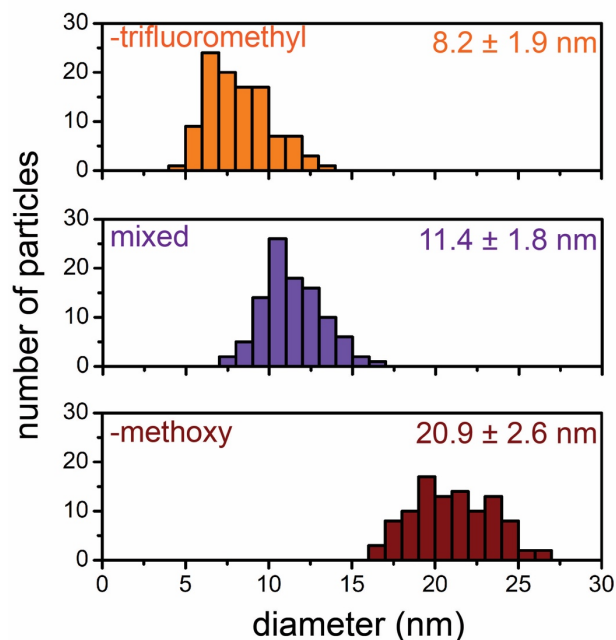


Figure S23. Nanorod size distributions for syntheses conducted with mixed modulators (1 equivalent of 4-methoxysalicylic acid and 1 equivalent of 4-trifluoromethylsalicylic acid) are compared to the size distribution for nanorods synthesized with either 1 equivalent of 4-methoxysalicylic acid or 4-trifluoromethylsalicylic acid.

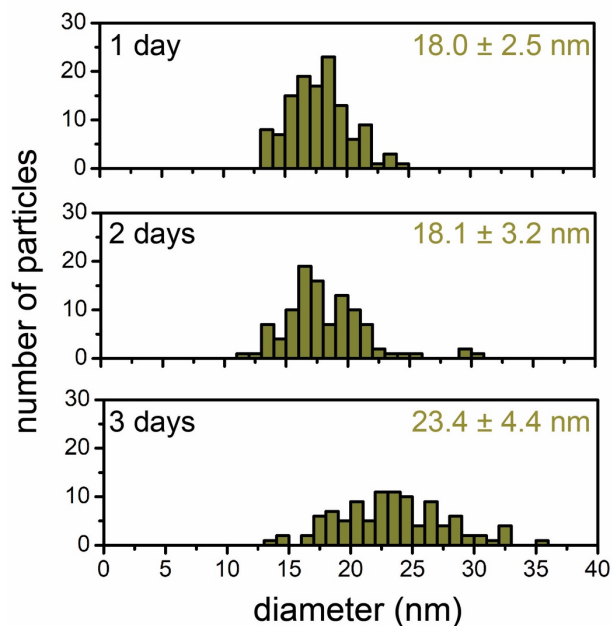


Figure S24. Nanorod size distributions for syntheses conducted with 1 equivalent of salicylic acid and reaction times 1, 2, or 3 days.

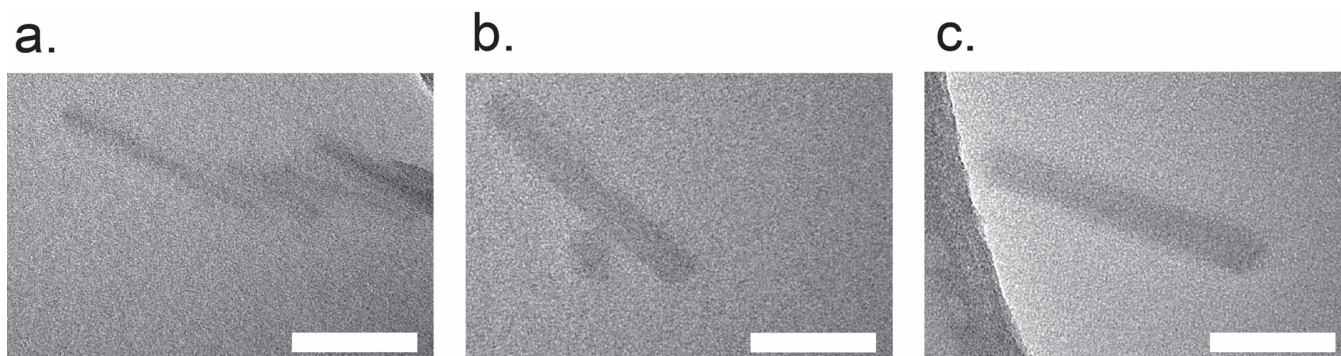


Figure S25. High-magnification TEM images of $\text{Co}_2(\text{dobdc})$ nanorods synthesized with 1 equivalent of (a) 4-trifluoromethylsalicylic acid, (b) salicylic acid, and (c) 4-methoxysalicylic acid. Scale bars: 50 nm.

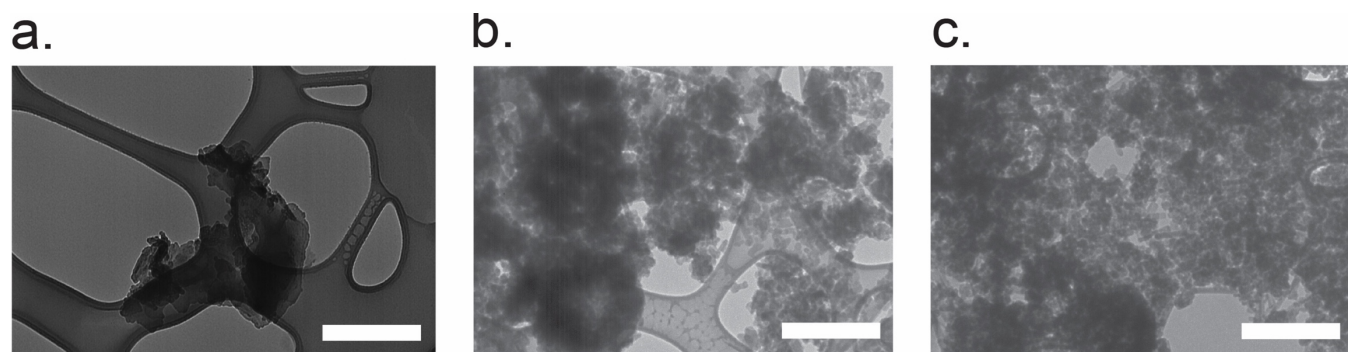


Figure S26. Representative TEM images of $\text{Co}_2(\text{dobdc})$ nanoparticles synthesized with 1 equivalent of (a) benzoic acid, (b) 4-trifluoromethylbenzoic acid, (c) 4-methoxybenzoic acid. Scale bars: 500 nm.

BET and External Surface Area

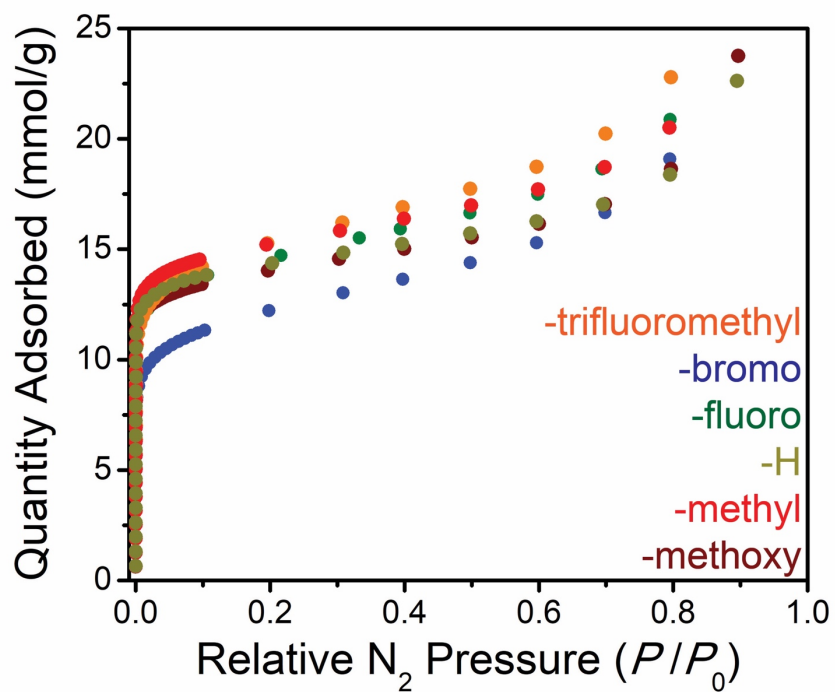


Figure S27. 77 K N_2 adsorption isotherms for $Co_2(dobdc)$ nanorods synthesized with 1 equivalent of various salicylic acid modulators.

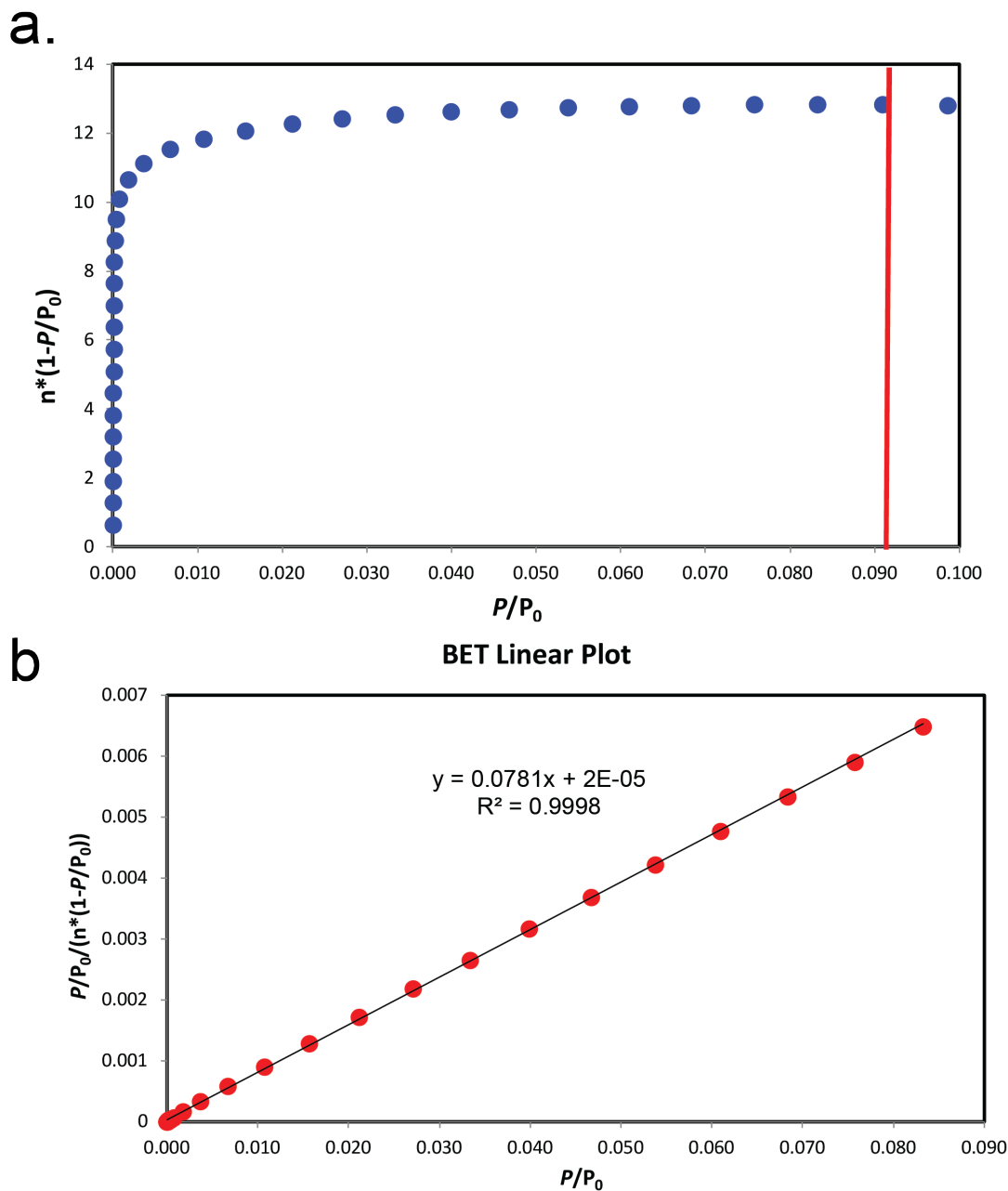


Figure S28. (a) Plot of $n \cdot (1 - P/P_0)$ vs. P/P_0 to determine the maximum P/P_0 used in the BET linear fit of 4-trifluoromethylsalicylic acid synthesized $\text{CO}_2(\text{dobdc})$ nanorods according to the first BET consistency criterion.³ (b) Plot of $P/P_0/(n \cdot (1 - P/P_0))$ vs. P/P_0 to determine the BET surface area for 4-trifluoromethylsalicylic acid $\text{CO}_2(\text{dobdc})$ nanorods. The slope of the best fit line for $P/P_0 < 0.082$ is 0.0781, and the y-intercept is 2×10^{-5} , which satisfies the second BET consistency criterion.³ This results in a saturation capacity of 14.0 mmol/g and a BET surface area of 1250 m^2/g .

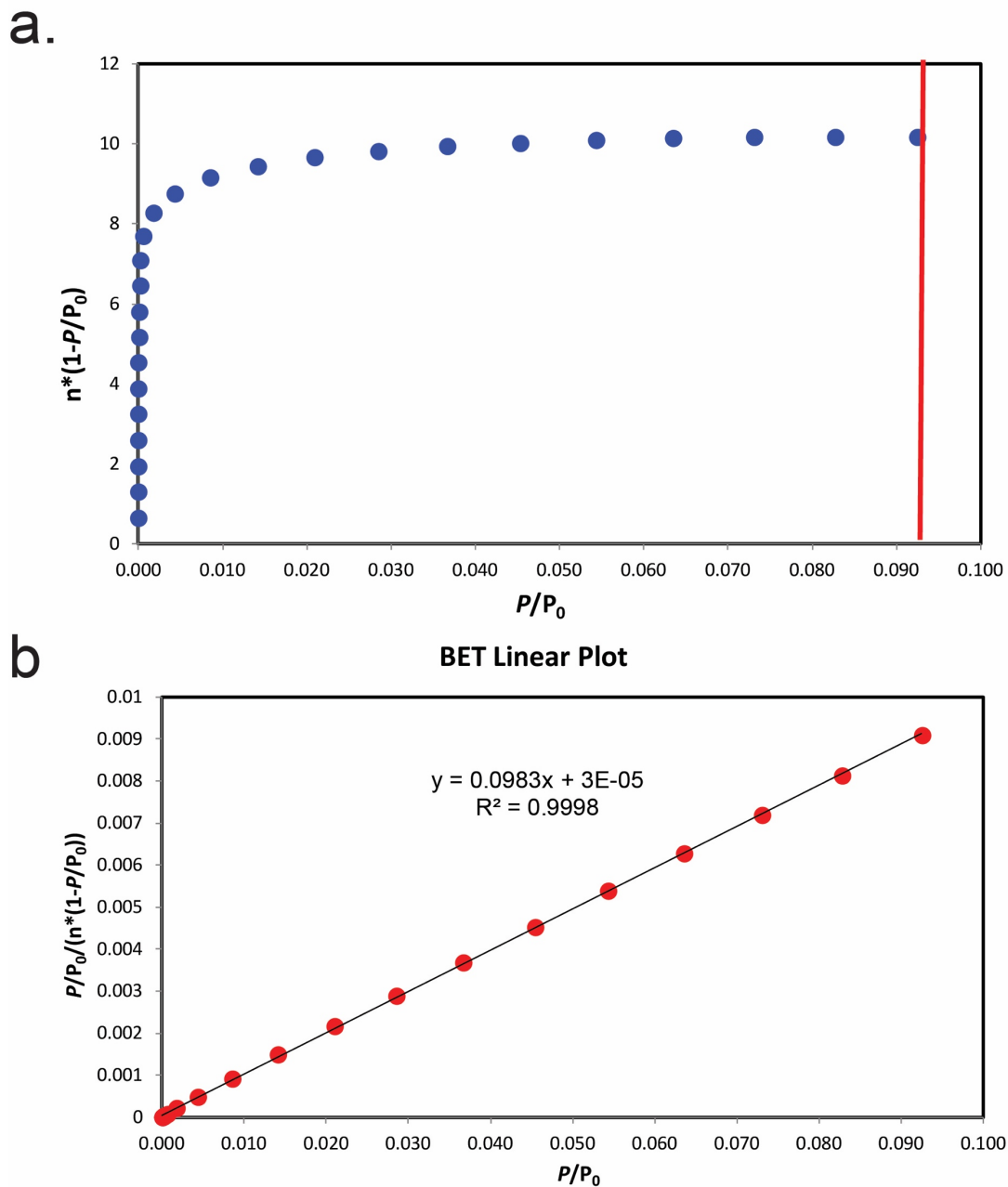


Figure S29. (a) Plot of $n \cdot (1 - P/P_0)$ vs. P/P_0 to determine the maximum P/P_0 used in the BET linear fit of 4-bromosalicylic acid synthesized $\text{Co}_2(\text{dobdc})$ nanorods according to the first BET consistency criterion.³ (b) Plot of $P/P_0/(n \cdot (1 - P/P_0))$ vs. P/P_0 to determine the BET surface area for 4-bromosalicylic acid $\text{Co}_2(\text{dobdc})$ nanorods. The slope of the best fit line for $P/P_0 < 0.092$ is 0.0983, and the y-intercept is 3×10^{-5} , which satisfies the second BET consistency criterion. This results in a saturation capacity of 11.2 mmol/g and a BET surface area of 993 m^2/g .³

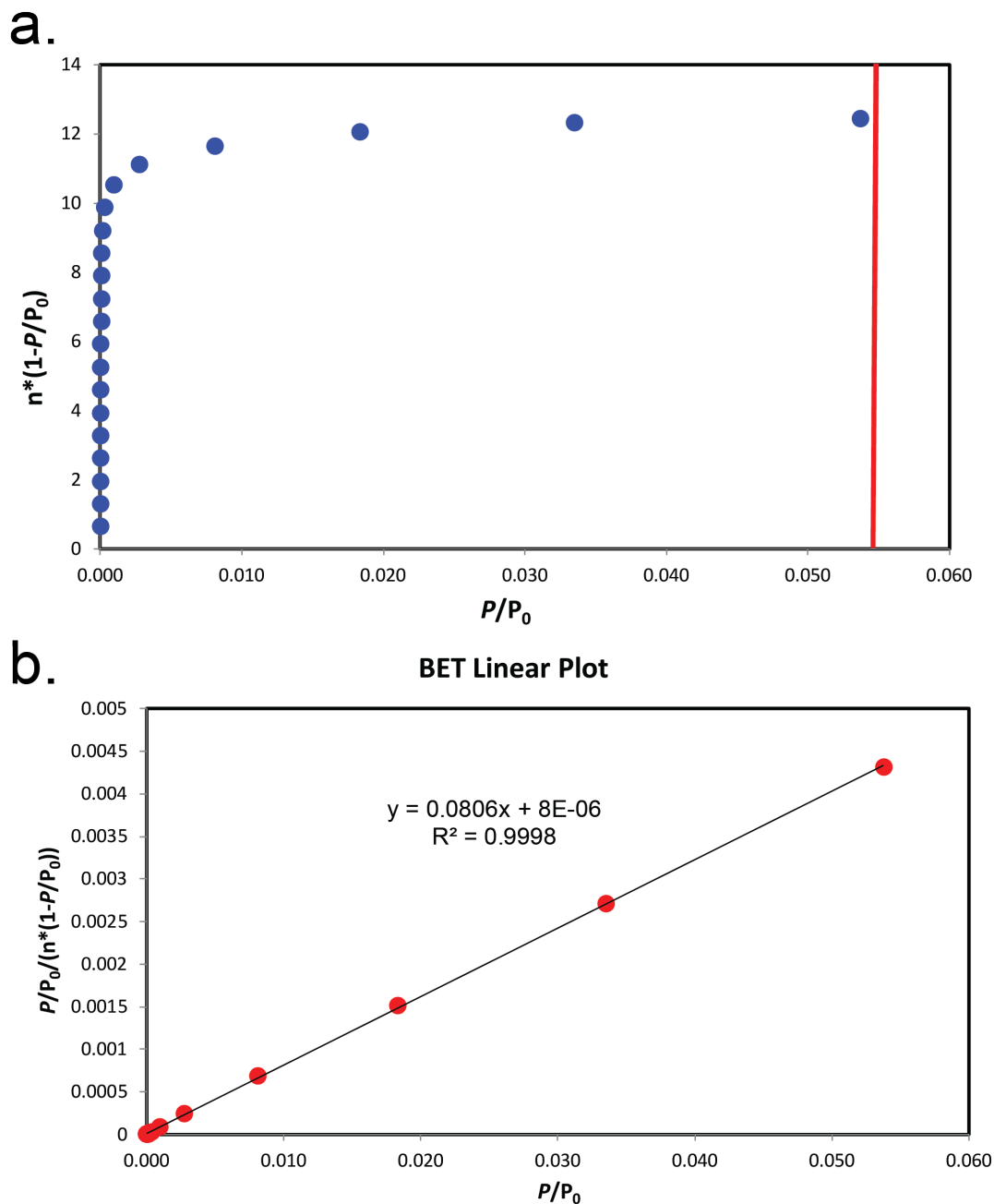


Figure S30. (a) Plot of $n^*(1 - P/P_0)$ vs. P/P_0 to determine the maximum P/P_0 used in the BET linear fit of 4-fluorosalicic acid synthesized $\text{Co}_2(\text{dobdc})$ nanorods according to the first BET consistency criterion.³ (b) Plot of $P/P_0/(n^*(1 - P/P_0))$ vs. P/P_0 to determine the BET surface area for 4-fluorosalicic acid $\text{Co}_2(\text{dobdc})$ nanorods. The slope of the best fit line for $P/P_0 < 0.061$ is 0.0806, and the y-intercept is 8×10^{-6} , which satisfies the second BET consistency criterion. This results in a saturation capacity of 13.1 mmol/g and a BET surface area of 1211 m^2/g .³

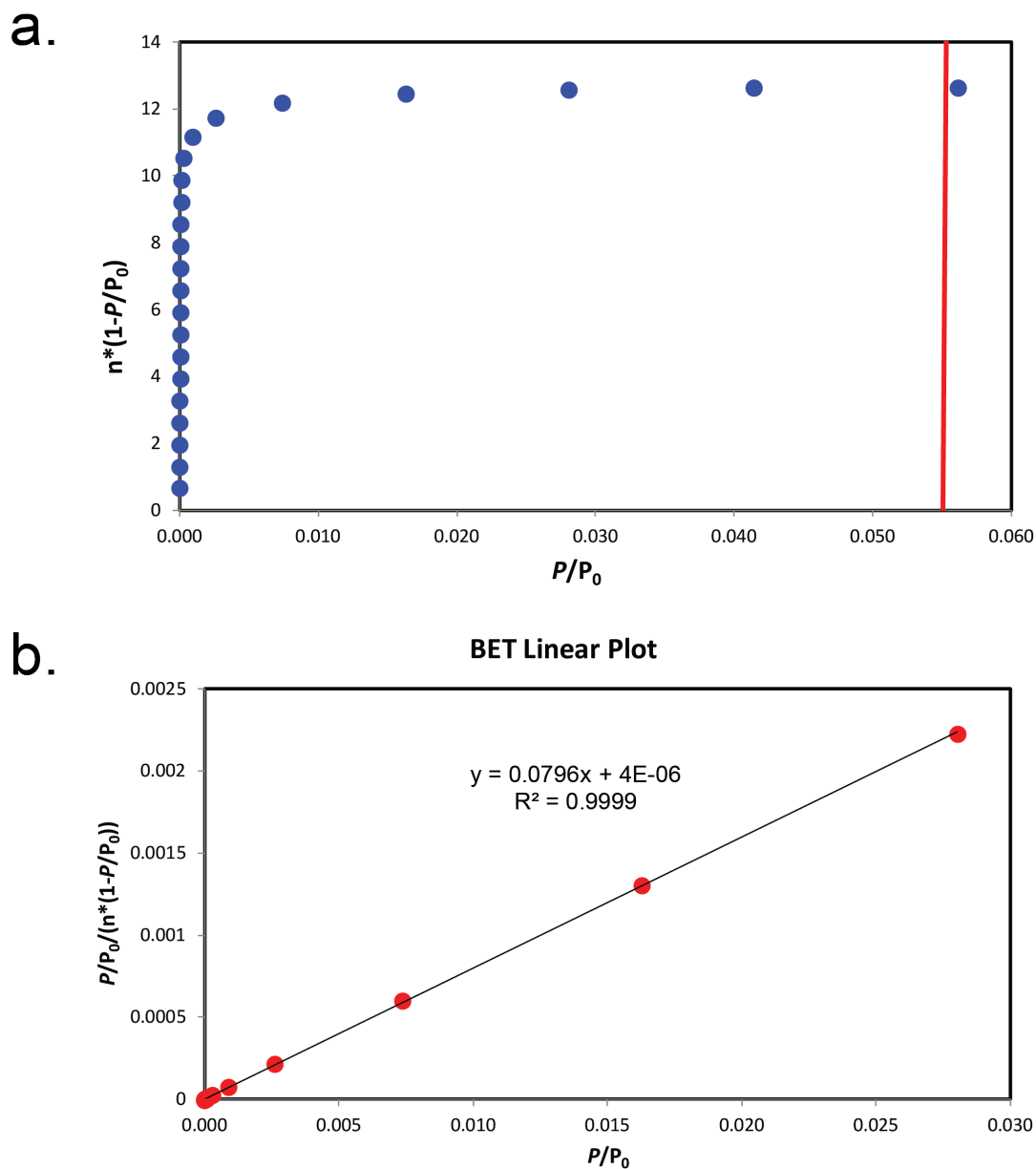


Figure S31. (a) Plot of $n \cdot (1 - P/P_0)$ vs. P/P_0 to determine the maximum P/P_0 used in the BET linear fit of salicylic acid synthesized $\text{Co}_2(\text{dobdc})$ nanorods according to the first BET consistency criterion.³ (b) Plot of $P/P_0/(n \cdot (1 - P/P_0))$ vs. P/P_0 to determine the BET surface area for salicylic acid $\text{Co}_2(\text{dobdc})$ nanorods. The slope of the best fit line for $P/P_0 < 0.061$ is 0.0796, and the y-intercept is 4×10^{-6} , which satisfies the second BET consistency criterion. This results in a saturation capacity of 13.3 mmol/g and a BET surface area of 1233 m^2/g .³

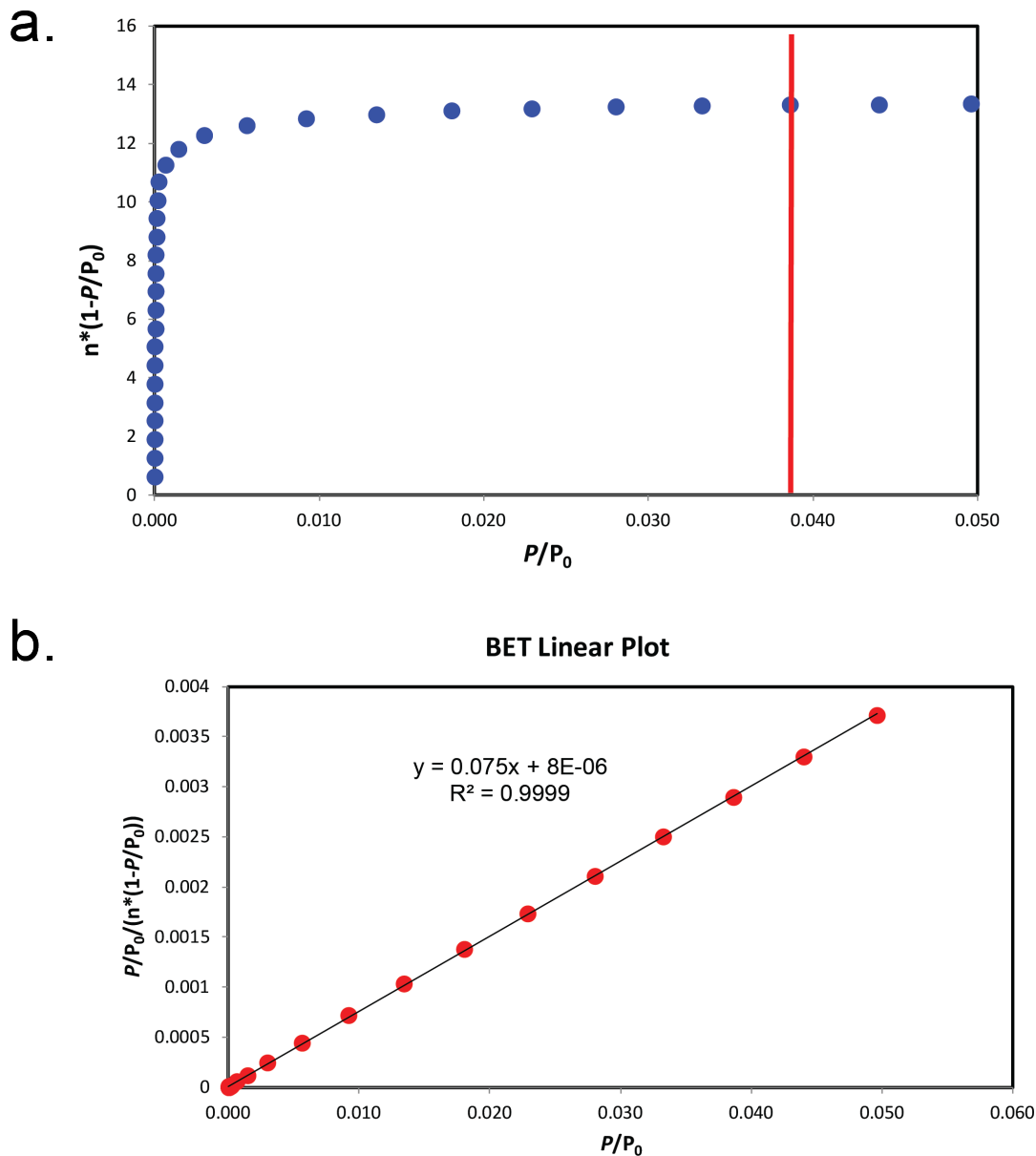


Figure S32. (a) Plot of $n \cdot (1 - P/P_0)$ vs. P/P_0 to determine the maximum P/P_0 used in the BET linear fit of 4-methylsalicylic acid synthesized $\text{Co}_2(\text{dobdc})$ nanorods according to the first BET consistency criterion.³ (b) Plot of $P/P_0 / (n \cdot (1 - P/P_0))$ vs. P/P_0 to determine the BET surface area for 4-methylsalicylic acid $\text{Co}_2(\text{dobdc})$ nanorods. The slope of the best fit line for $P/P_0 < 0.05$ is 0.075, and the y-intercept is 8×10^{-6} , which satisfies the second BET consistency criterion. This results in a saturation capacity of 14.0 mmol/g and a BET surface area of 1300 m^2/g .³

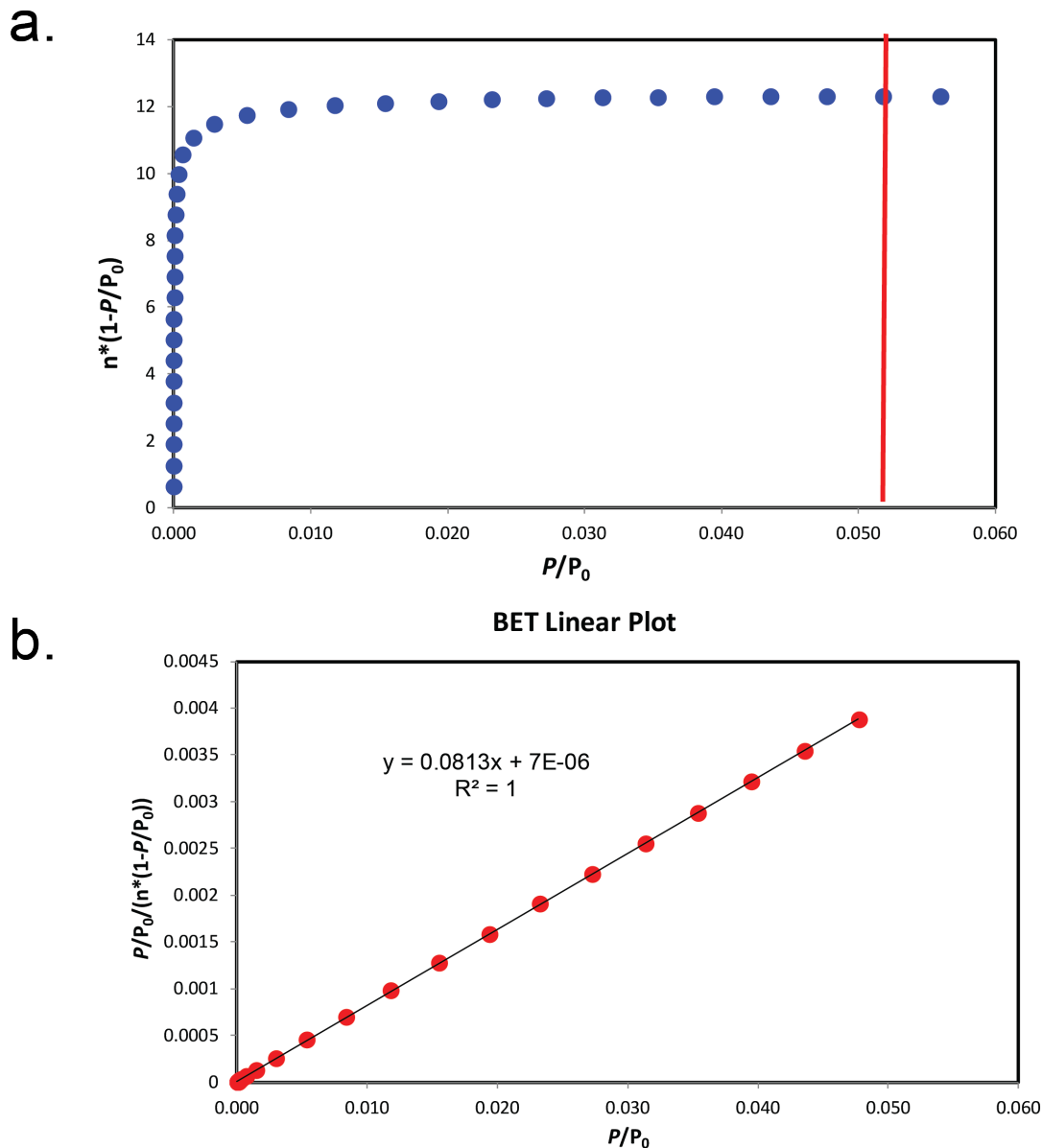


Figure S33. (a) Plot of $n \cdot (1 - P/P_0)$ vs. P/P_0 to determine the maximum P/P_0 used in the BET linear fit of 4-methoxysalicylic acid synthesized $\text{Co}_2(\text{dobdc})$ nanorods according to the first BET consistency criterion.³ (b) Plot of $P/P_0/(n \cdot (1 - P/P_0))$ vs. P/P_0 to determine the BET surface area for 4-methoxysalicylic acid $\text{Co}_2(\text{dobdc})$ nanorods. The slope of the best fit line for $P/P_0 < 0.05$ is 0.0813, and the y-intercept is 7×10^{-6} , which satisfies the second BET consistency criterion. This results in a saturation capacity of 12.9 mmol/g and a BET surface area of $1199 \text{ m}^2/\text{g}$.³

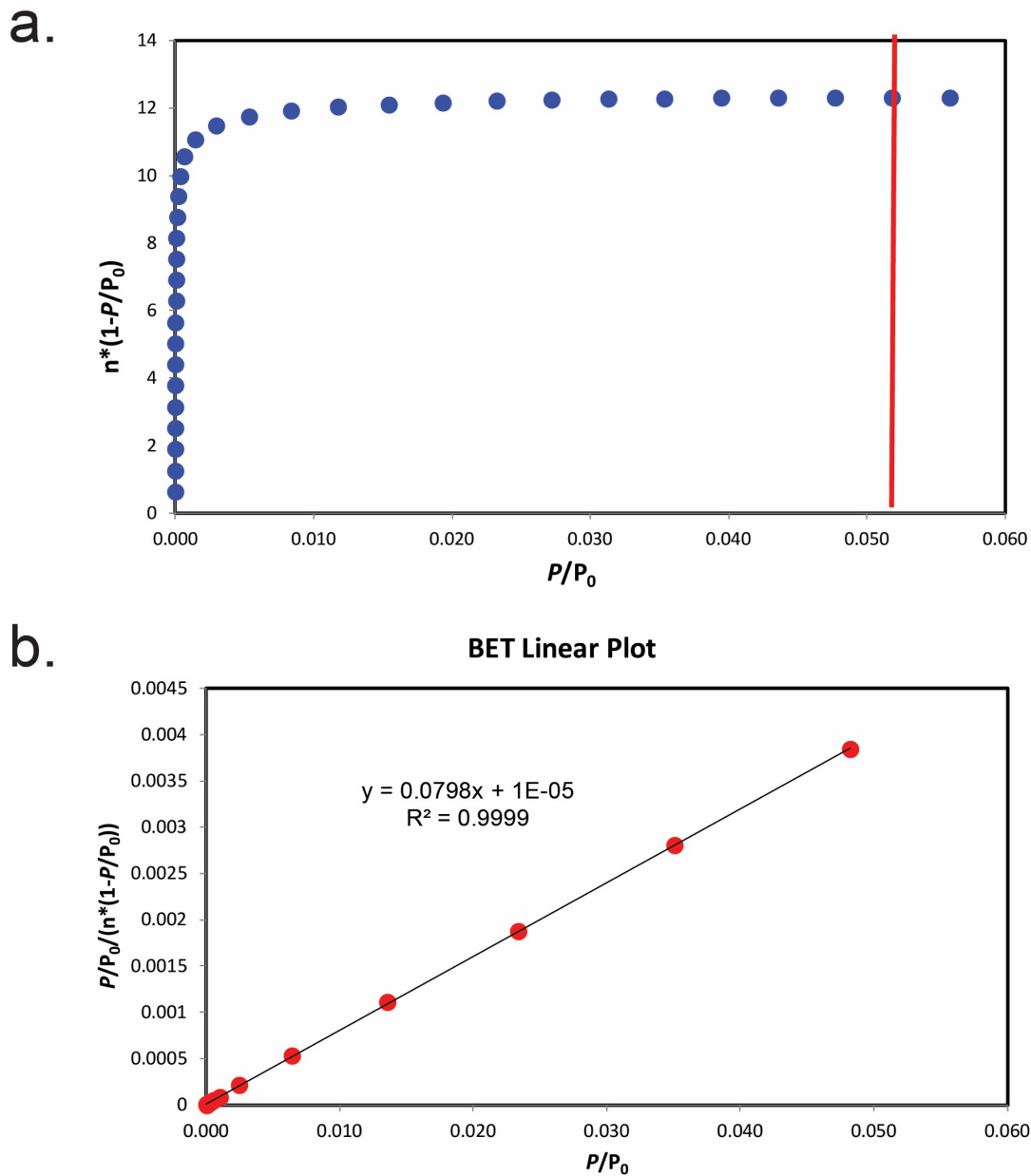


Figure S34. (a) Plot of $n \cdot (1 - P/P_0)$ vs. P/P_0 to determine the maximum P/P_0 used in the BET linear fit of surface exchanged $\text{Co}_2(\text{dobdc})$ nanorods according to the first BET consistency criterion.³ (b) Plot of $P/P_0 / (n \cdot (1 - P/P_0))$ vs. P/P_0 to determine the BET surface area for surface exchanged $\text{Co}_2(\text{dobdc})$ nanorods. The slope of the best fit line for $P/P_0 < 0.048$ is 0.0798, and the y-intercept is 1×10^{-5} , which satisfies the second BET consistency criterion. This results in a saturation capacity of 13.1 mmol/g and a BET surface area of 1222 m^2/g .³

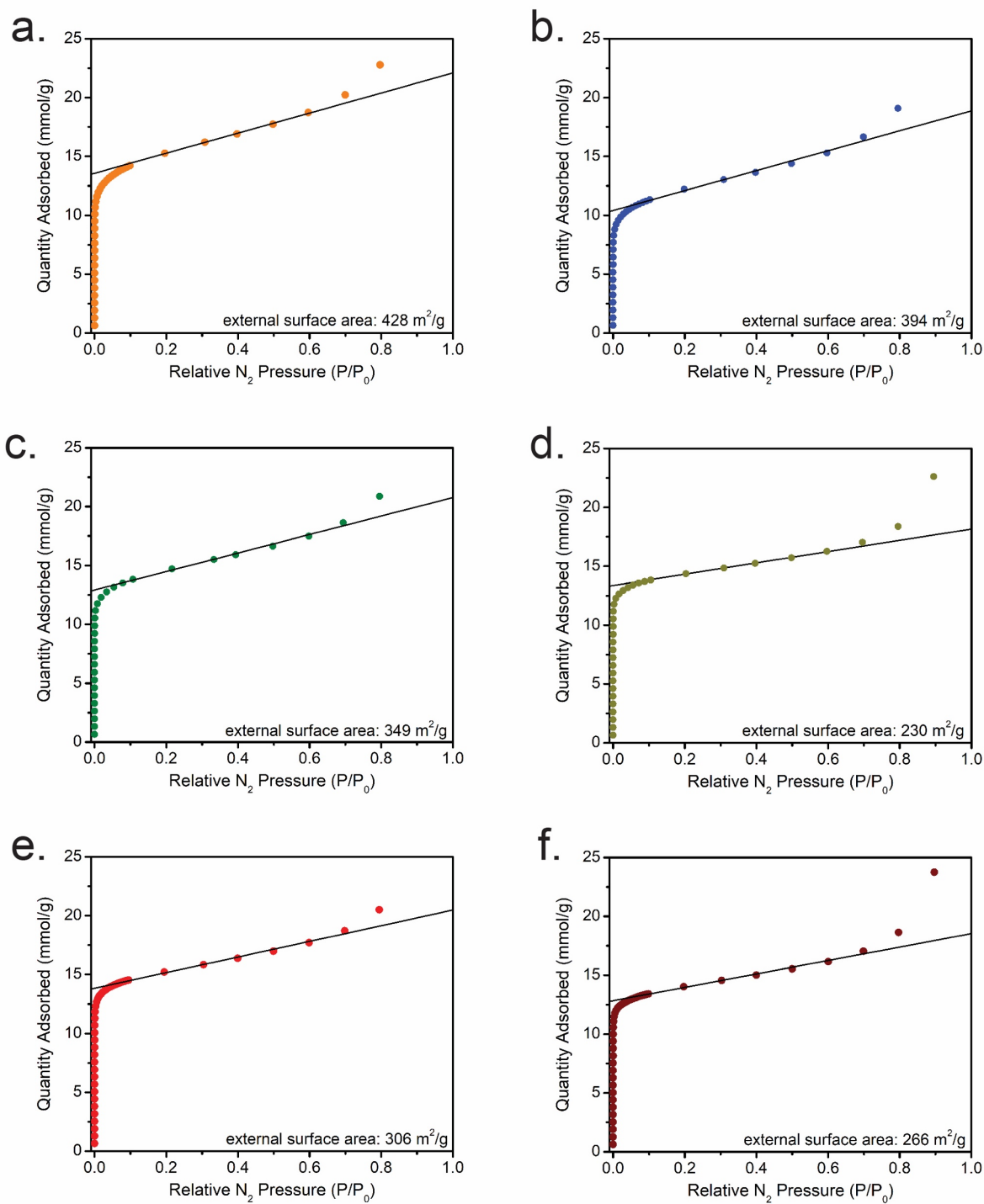


Figure S35. External surface area analysis by the t-plot method using the Harkins and Jura thickness curve and a fitted range of 4.8 to 13.2 Å for $\text{Co}_2(\text{dobdc})$ nanorods synthesized with 1 equivalent of (a) 4-trifluoromethylsalicylic acid (b) 4-bromosalicylic acid, (c) 4-fluorosalicylic acid, (d) salicylic acid, (e) 4-methylsalicylic acid, and (f) 4-methoxysalicylic acid.

CO₂ Adsorption Isotherms

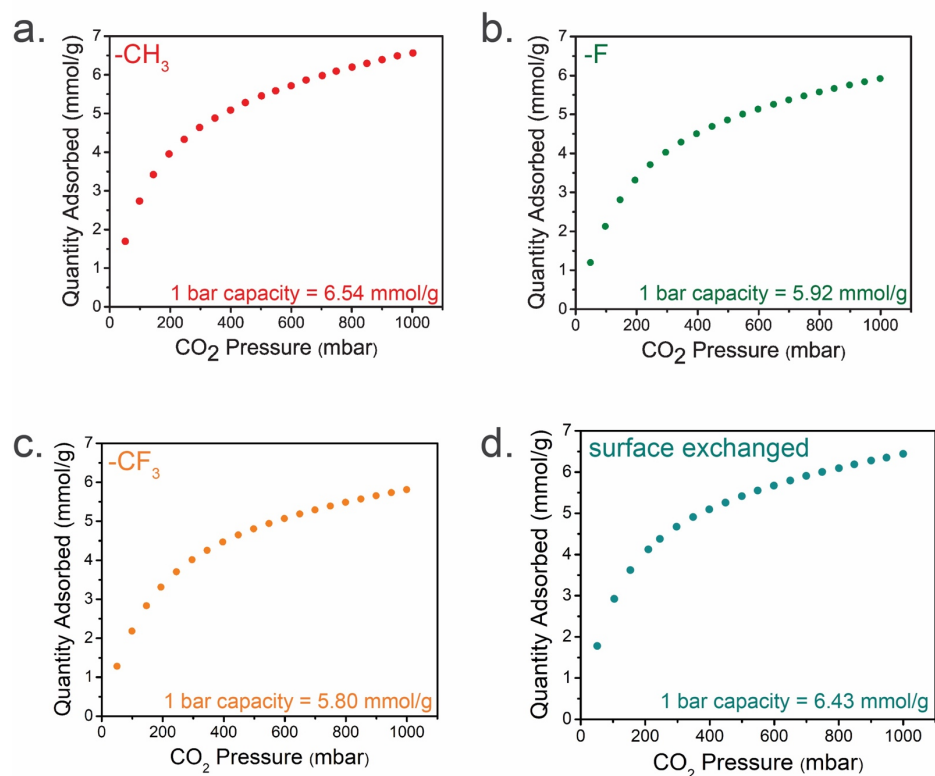


Figure S36. CO₂ adsorption isotherms at 25 °C for Co₂(dobdc) nanorods synthesized with (a) 1 equivalent of 4-methoxysalicylic acid, (b) 1 equivalent of 4-fluorosalicylic acid, (c), 1 equivalent of 4-trifluoromethylsalicylic acid and (d) 1 equivalent of salicylic acid followed by surface exchange with 4-trifluoromethylsalicylic acid.

Quantification of Bound Modulator

T1 Analysis

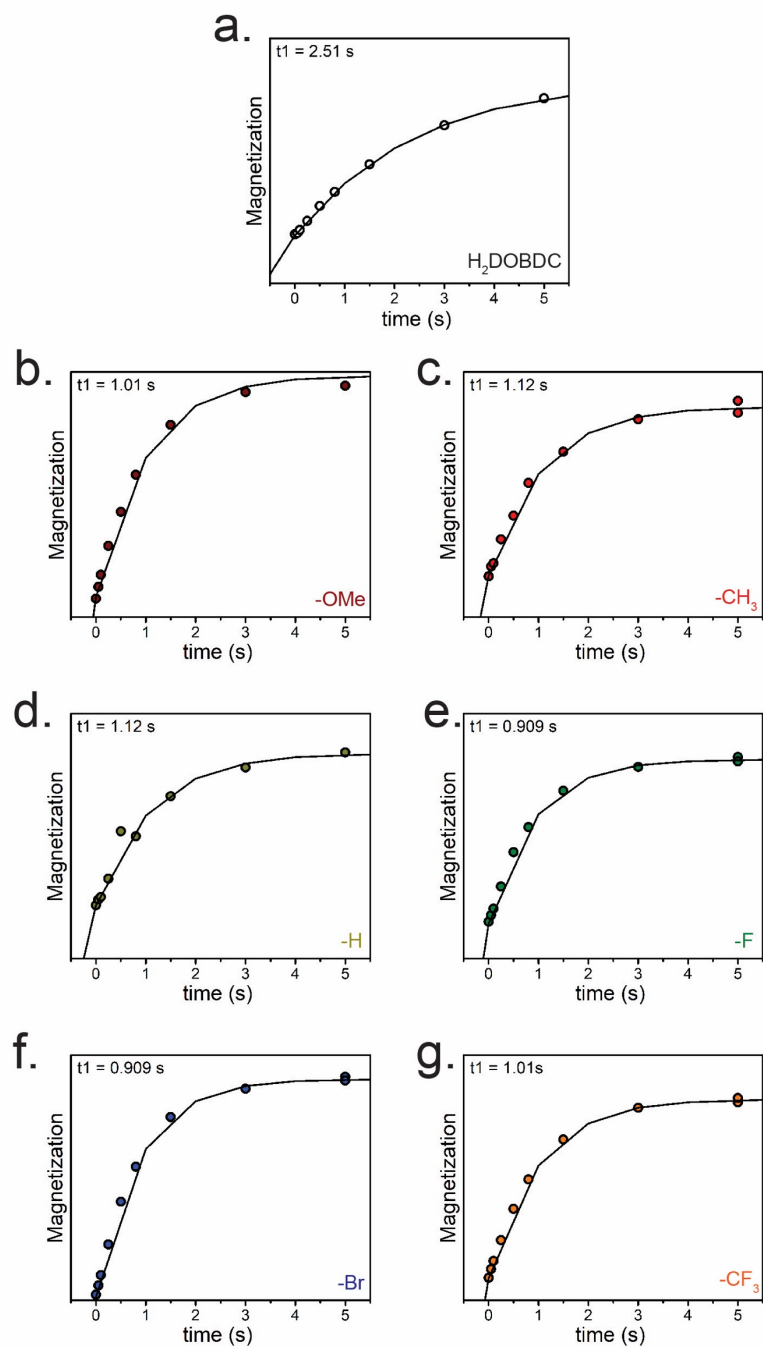


Figure S37. T_1 values for a) H_2dobdc , b) 4-methoxysalicylic acid, c) 4-methylsalicylic acid, d) salicylic acid, e) 4-fluorosalicylic acid, f) 4-bromosalicylic acid and g) 4-trifluoromethylsalicylic acid.

Nuclear Magnetic Resonance Spectroscopy (NMR)

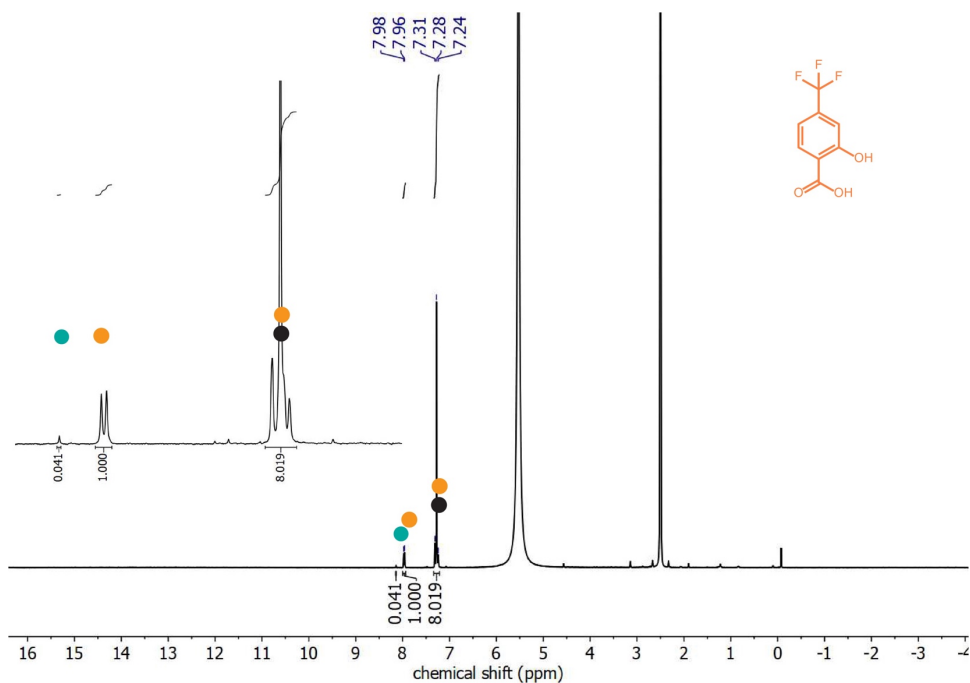


Figure S38. ¹H-NMR (400 MHz, DMSO-d₆) of digested Co₂(dobdc) nanorods synthesized with 1 equivalent of 4-trifluoromethylsalicylic acid. Orange dots correspond to 4-trifluoromethylsalicylic acid protons. The black dot corresponds to H₂dobdc protons, and the teal dot corresponds to formate protons.

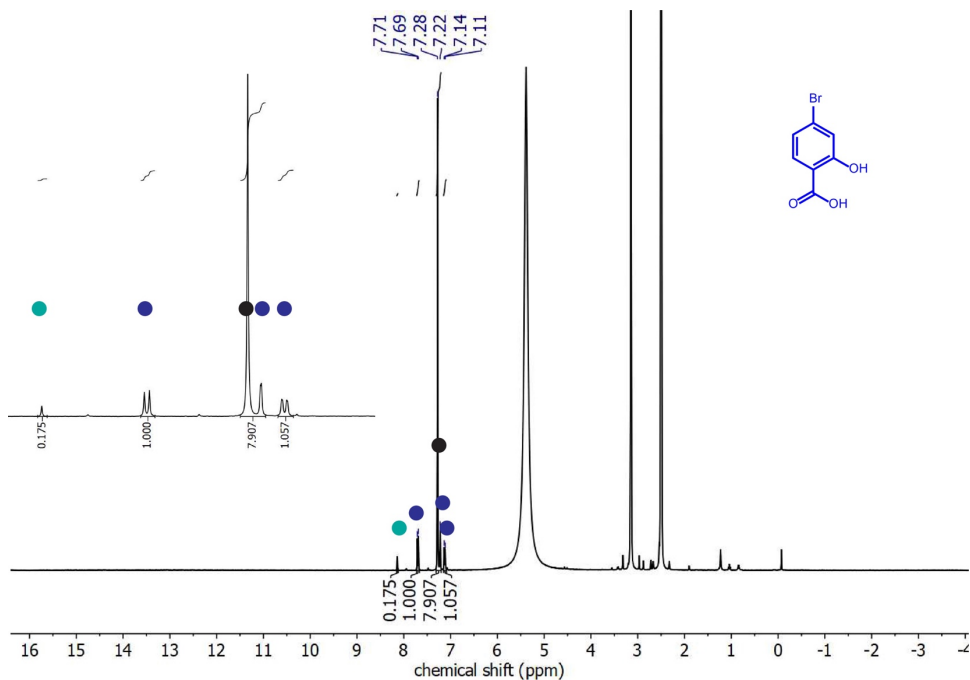


Figure S39. ¹H-NMR (400 MHz, DMSO-d₆) of Co₂(dobdc) nanorods synthesized with 1 equivalent of 4-bromosalicylic acid. Blue dots correspond to 4-bromosalicylic acid protons. The black dot corresponds to H₂dobdc protons, and the teal dot corresponds to formate protons.

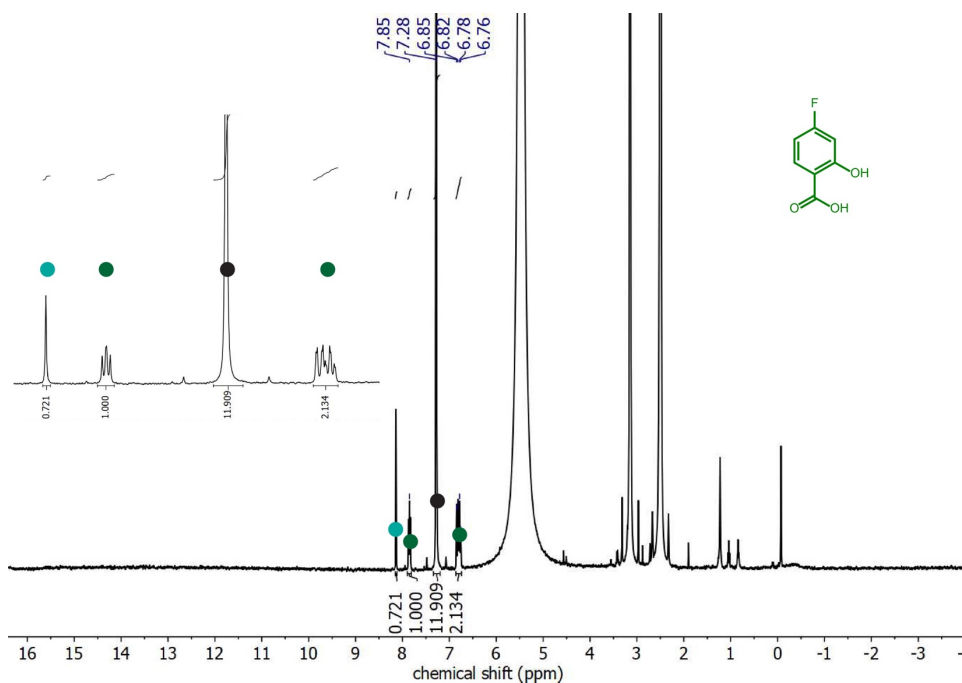


Figure S40. ¹H-NMR (400 MHz, DMSO-d₆) of Co₂(dobdc) nanorods synthesized with 1 equivalent of 4-fluorosalicic acid. Green dots correspond to 4-fluorosalicic acid protons. The black dot corresponds to H₂dobdc protons, and the teal dot corresponds to formate protons.

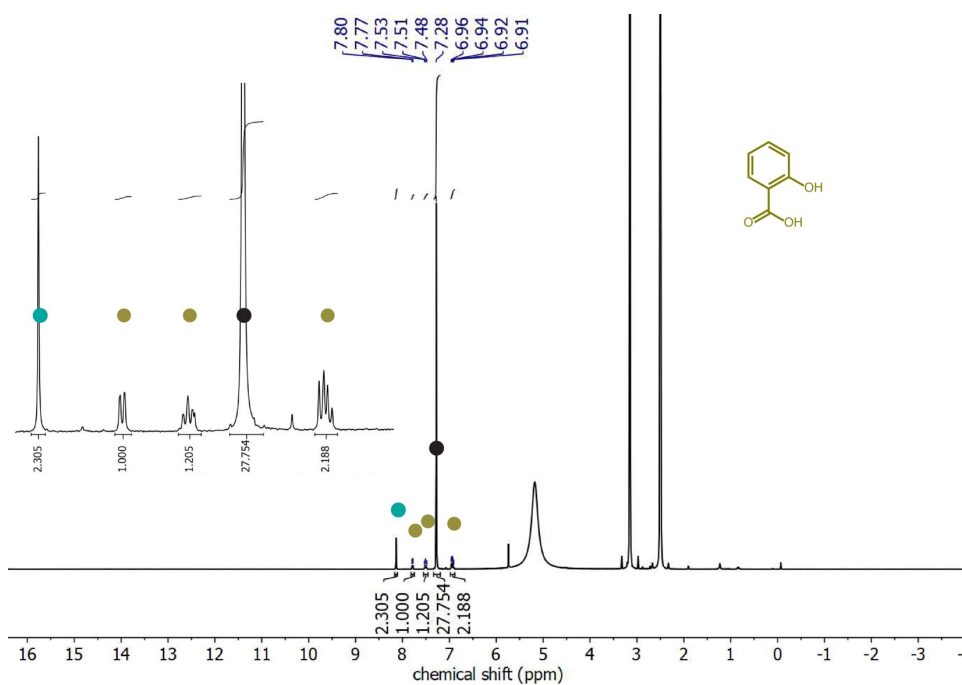


Figure S41. ¹H-NMR (400 MHz, DMSO-d₆) of Co₂(dobdc) nanorods synthesized with 1 equivalent of salicylic acid. Dark yellow dots correspond to salicylic acid protons. The black dot corresponds to H₂dobdc protons, and the teal dot corresponds to formate protons.

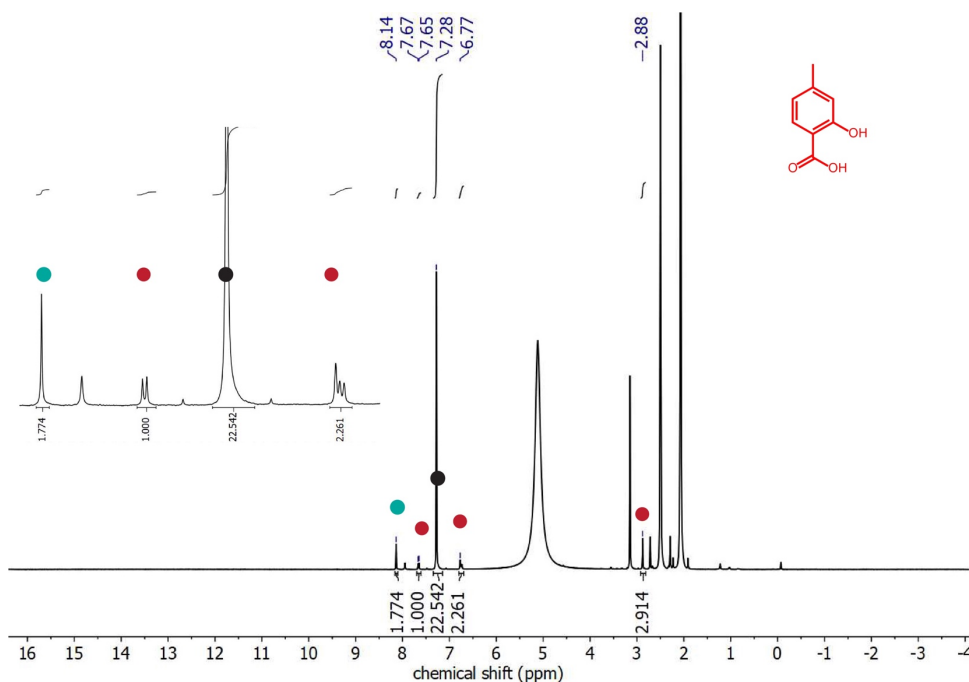


Figure S42. ¹H-NMR (400 MHz, DMSO-d₆) of Co₂(dobdc) nanorods synthesized with 1 equivalent of 4-methylsalicylic acid. Red dots correspond to 4-methylsalicylic acid protons. The black dot corresponds to H₂dobdc protons, and the teal dot corresponds to formate protons.

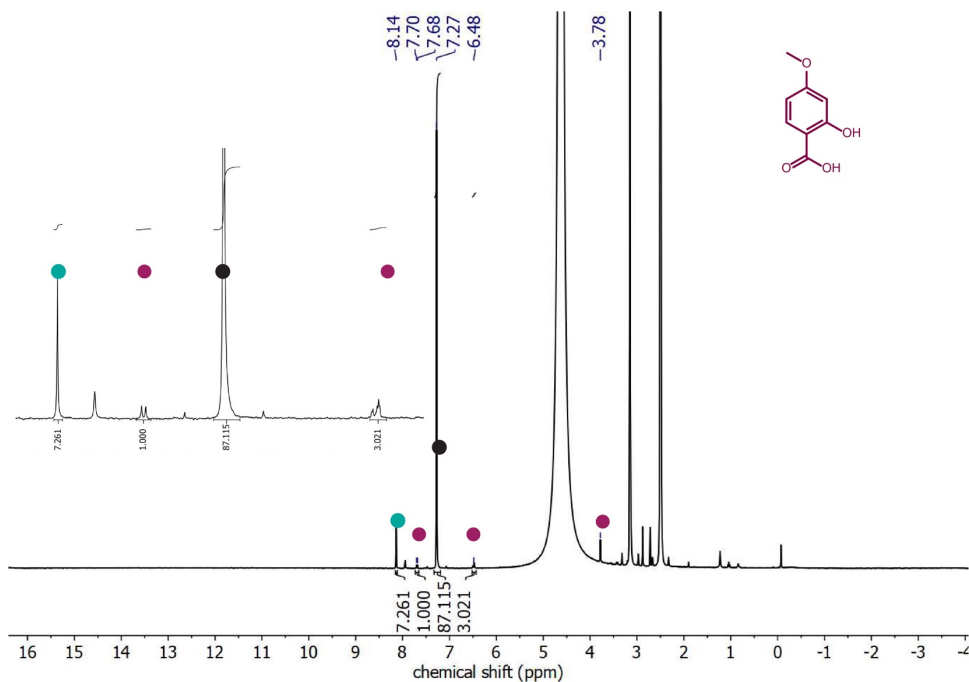


Figure S43. ¹H-NMR (400 MHz, DMSO-d₆) of Co₂(dobdc) nanorods synthesized with 1 equivalent of 4-methoxysalicylic acid. Light purple dots correspond to 4-methoxysalicylic acid protons. The black dot corresponds to H₂dobdc protons, and the teal dot corresponds to formate protons.

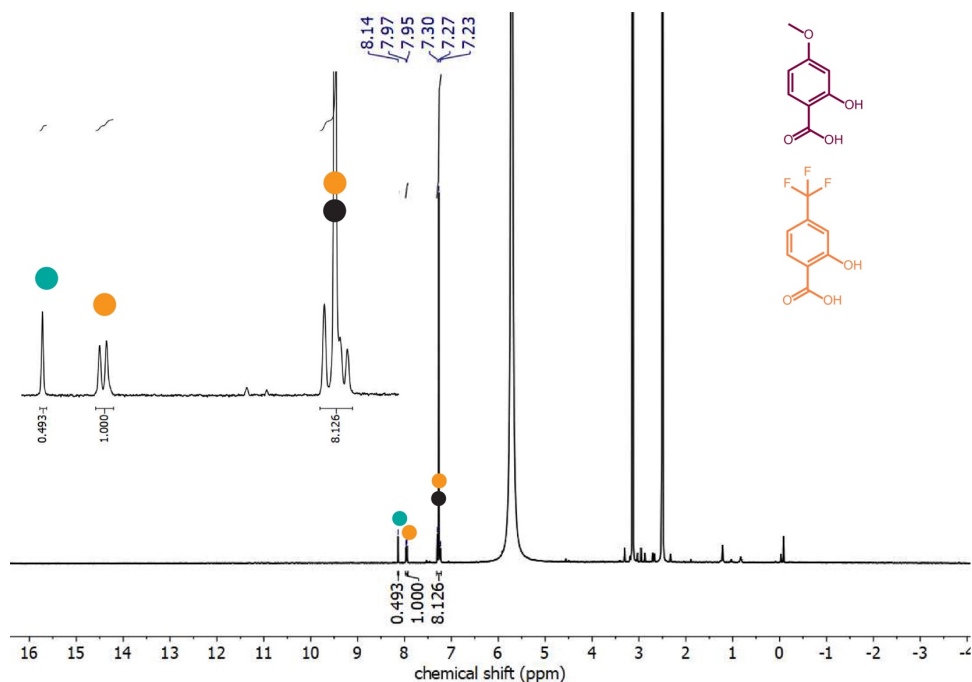


Figure S44. $^1\text{H-NMR}$ (400 MHz, DMSO- d_6) of $\text{Co}_2(\text{dobdc})$ synthesized with a mixed modulator system (1 equivalent of 4-trifluoromethylbenzoic acid and 1 equivalent of 4-methoxysalicylic acid). Orange dots correspond to 4-trifluoromethylsalicylic acid protons. The black dot corresponds to H_2dobdc protons, and the teal dot corresponds to formate protons.

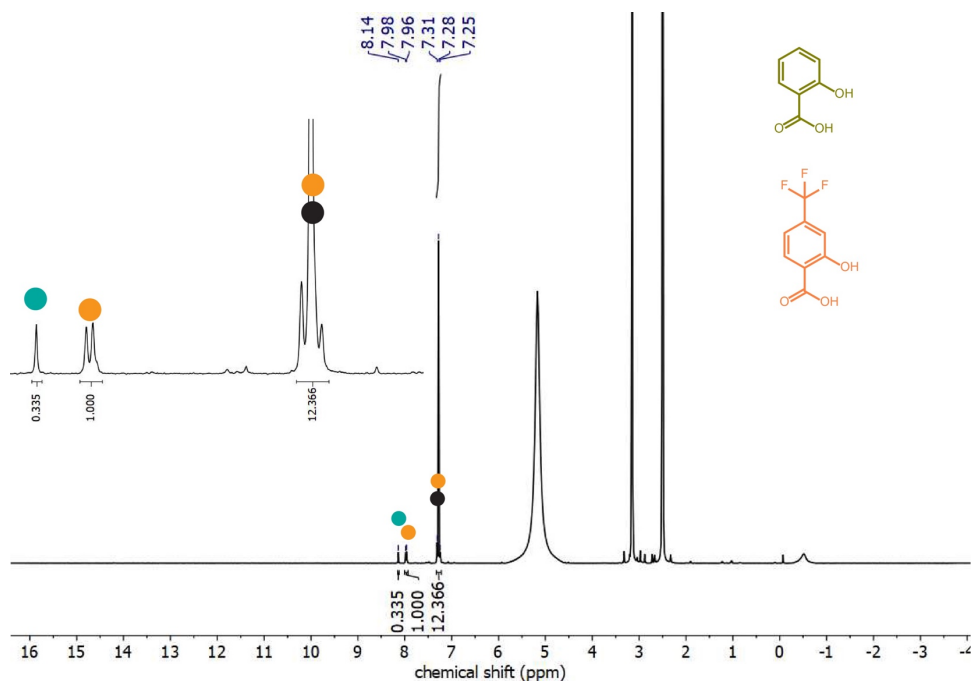


Figure S45. $^1\text{H-NMR}$ (400 MHz, DMSO- d_6) of $\text{Co}_2(\text{dobdc})$ synthesized with 1 equivalent of salicylic acid then surface exchanged with 2 equivalents of 4-trifluoromethylsalicylic acid. Orange dots correspond to 4-trifluoromethylsalicylic acid protons. The black dot corresponds to H_2dobdc protons, and the teal dot corresponds to formate protons.

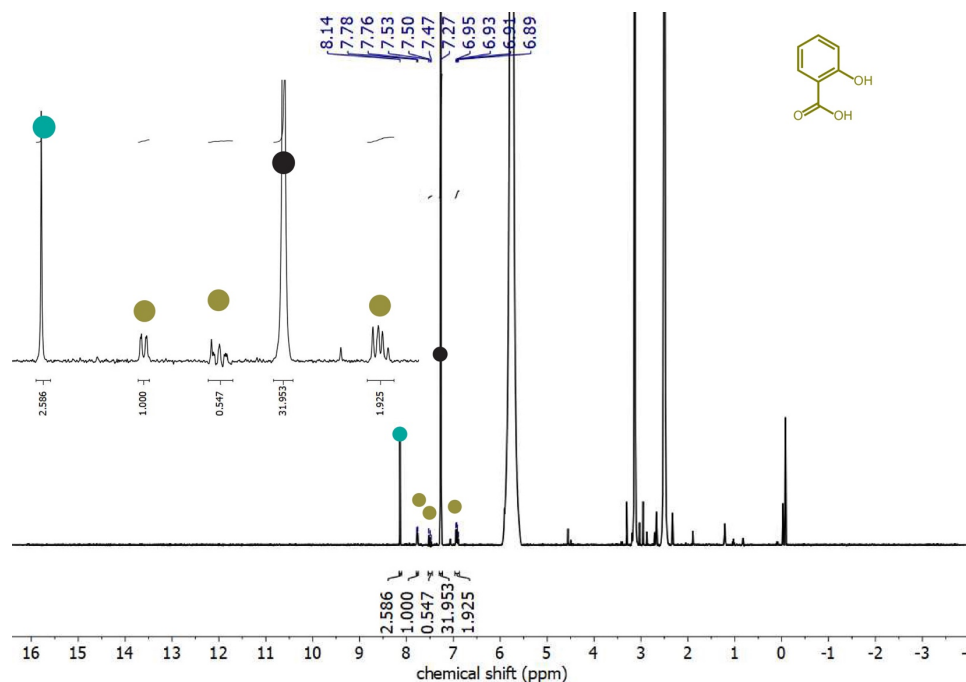


Figure S46. ¹H-NMR (400 MHz, DMSO-d₆) of Co₂(dobdc) nanorods synthesized with 1 equivalent of salicylic acid and a reaction time of 2 days. Dark yellow dots correspond to salicylic acid protons. The black dot corresponds to H₂dobdc protons, and the teal dot corresponds to formate protons.

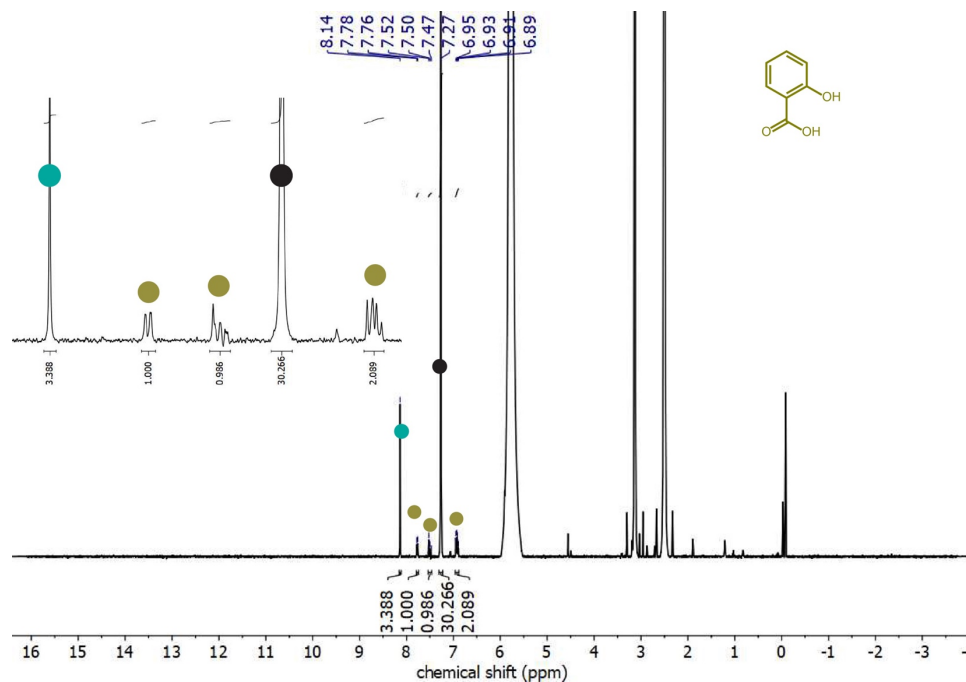


Figure S47. ¹H-NMR (400 MHz, DMSO-d₆) of Co₂(dobdc) nanorods synthesized with 1 equivalent of salicylic acid and a reaction time of 3 days. Dark yellow dots correspond to salicylic acid protons. The black dot corresponds to H₂dobdc protons, and the teal dot corresponds to formate protons.

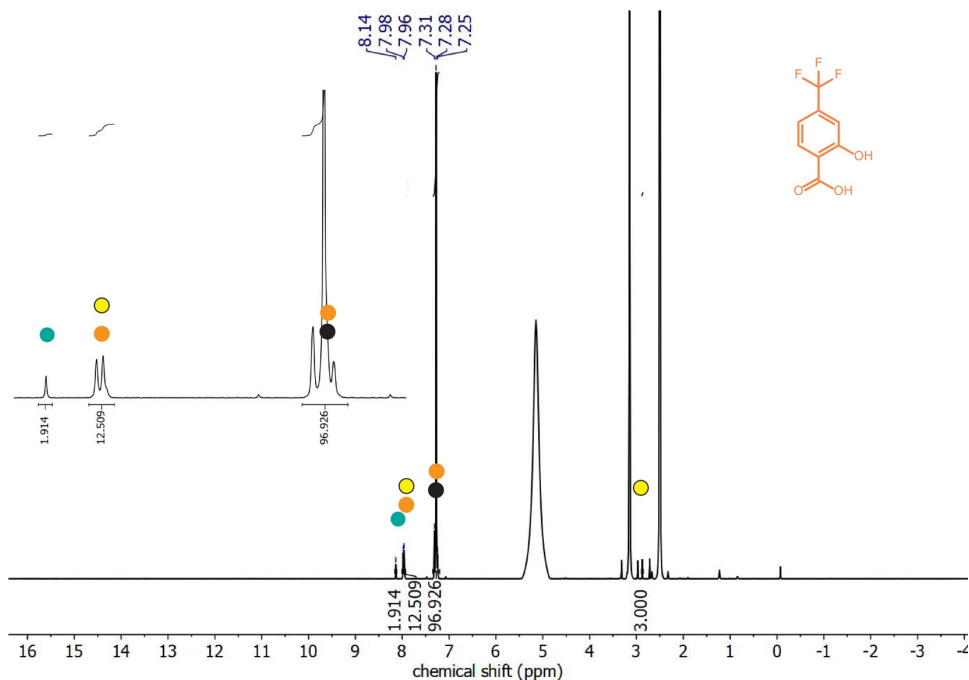


Figure S48. $^1\text{H-NMR}$ (400 MHz, DMSO-d_6) of $\text{Co}_2(\text{dobdc})$ nanorods synthesized with 1.5 equivalents of 4-trifluoromethylsalicylic acid. Orange dots correspond to 4-trifluoromethylsalicylic acid protons. The black dot corresponds to H_2dobdc protons. The yellow dot corresponds to DMF, and the teal dot corresponds to formate protons.

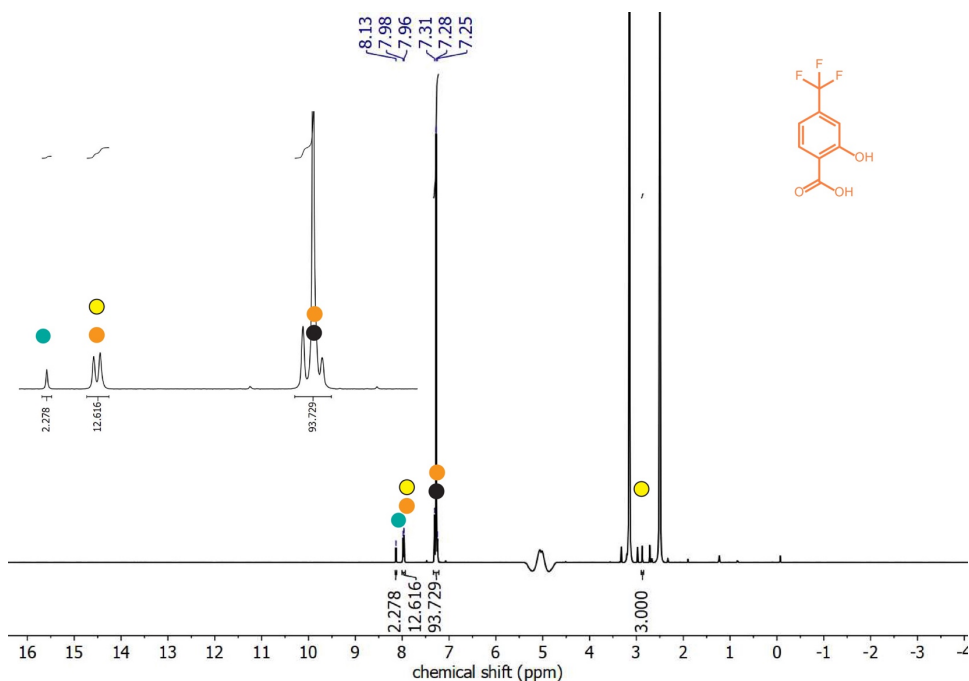


Figure S49. $^1\text{H-NMR}$ (400 MHz, DMSO-d_6) of $\text{Co}_2(\text{dobdc})$ nanorods synthesized with 2 equivalents of 4-trifluoromethylsalicylic acid. Orange dots correspond to 4-trifluoromethylsalicylic acid protons. The black dot corresponds to H_2dobdc protons. The yellow dot corresponds to DMF, and the teal dot corresponds to formate protons.

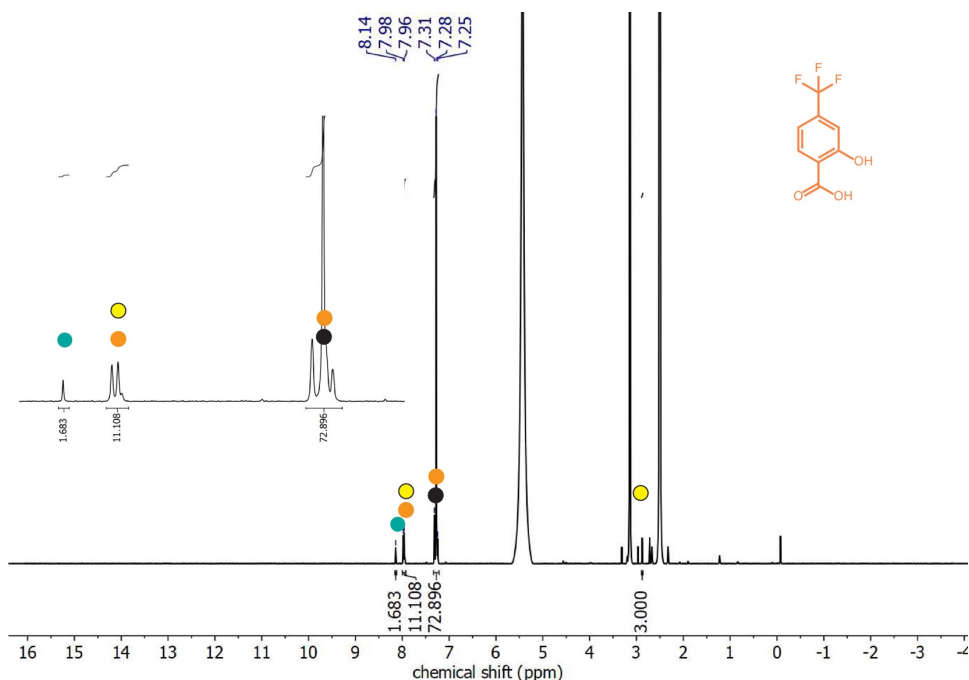


Figure S50. ¹H-NMR (400 MHz, DMSO-d₆) of Co₂(dobdc) nanorods synthesized with 3 equivalents of 4-trifluoromethylsalicylic acid. Orange dots correspond to 4-trifluoromethylsalicylic acid protons. The black dot represents H₂dobdc protons. The yellow dot corresponds to DMF, and the teal dot corresponds to formate protons.

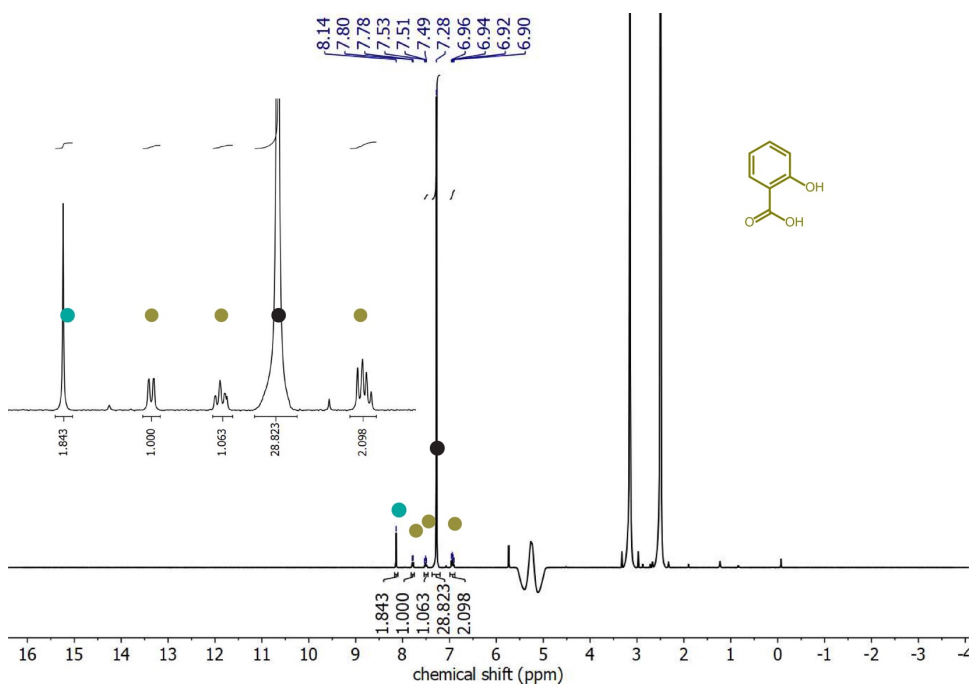


Figure S51. ¹H-NMR (400 MHz, DMSO-d₆) of Co₂(dobdc) nanorods synthesized with 1.5 equivalents of salicylic acid. Dark yellow dots correspond to salicylic acid protons. The black dot corresponds to H₂dobdc protons, and the teal dot corresponds to formate protons.

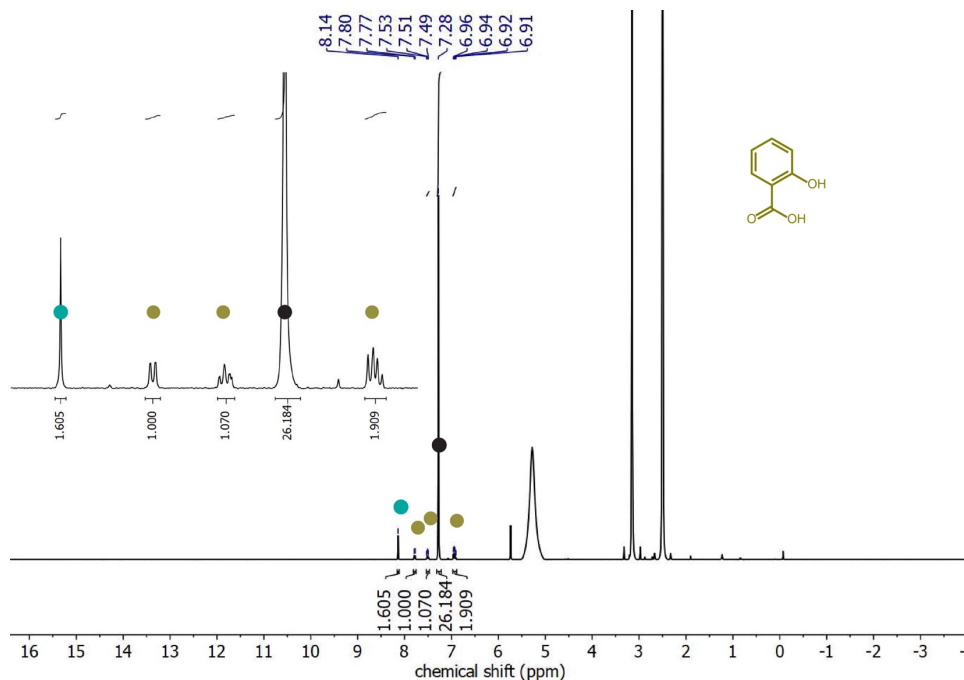


Figure S52. ¹H-NMR (400 MHz, DMSO-d₆) of Co₂(dobdc) nanorods synthesized with 2 equivalents of salicylic acid. Dark yellow dots correspond to salicylic acid protons. The black dot corresponds to H₂dobdc protons, and the teal dot corresponds to formate protons.

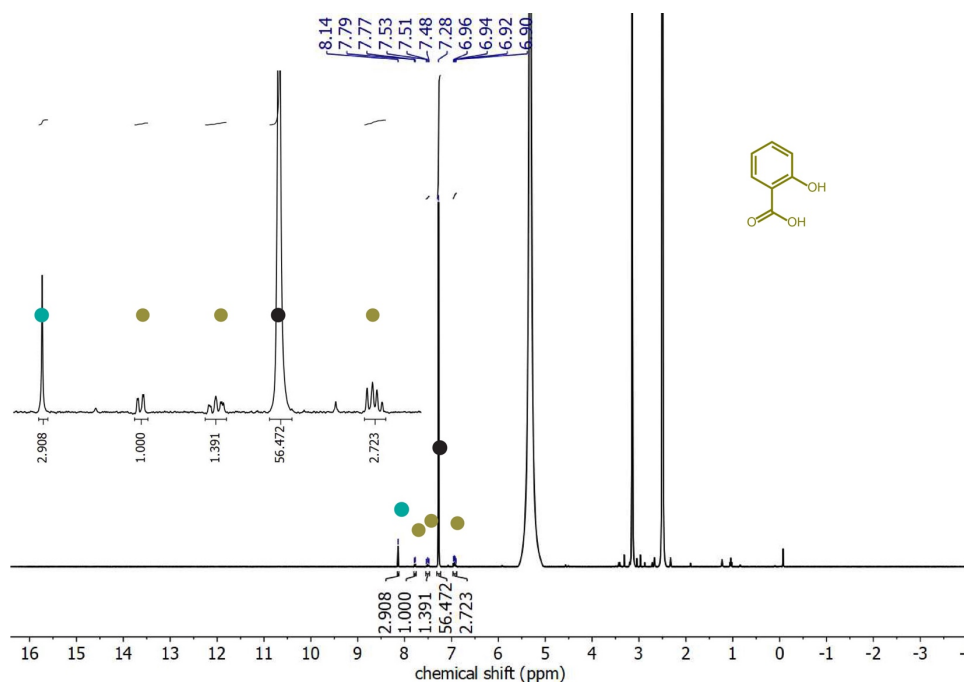


Figure S53. ¹H-NMR (400 MHz, DMSO-d₆) of Co₂(dobdc) nanorods synthesized with 3 equivalents of salicylic acid. Dark yellow dots correspond to salicylic acid protons. The black dot corresponds to H₂dobdc protons, and the teal dot corresponds to formate protons.

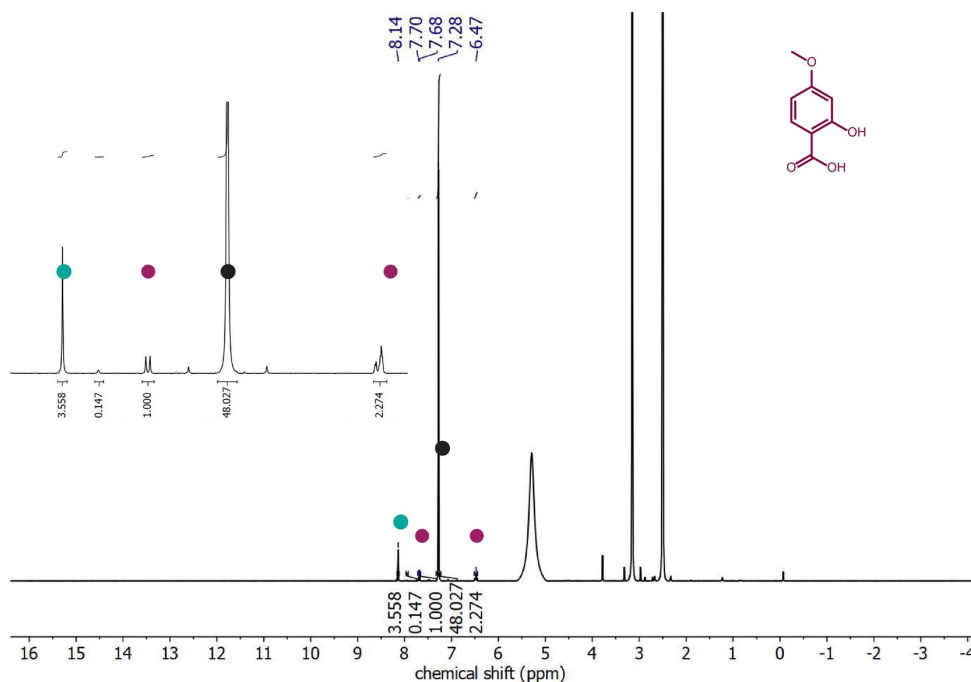


Figure S54. ¹H-NMR (400 MHz, DMSO-d₆) of Co₂(dobdc) nanorods synthesized with 1.5 equivalents of 4-methoxysalicylic acid. Light purple dots correspond to 4-methoxysalicylic acid protons. The black dot corresponds to H₂dobdc protons, and the teal dot corresponds to formate protons.

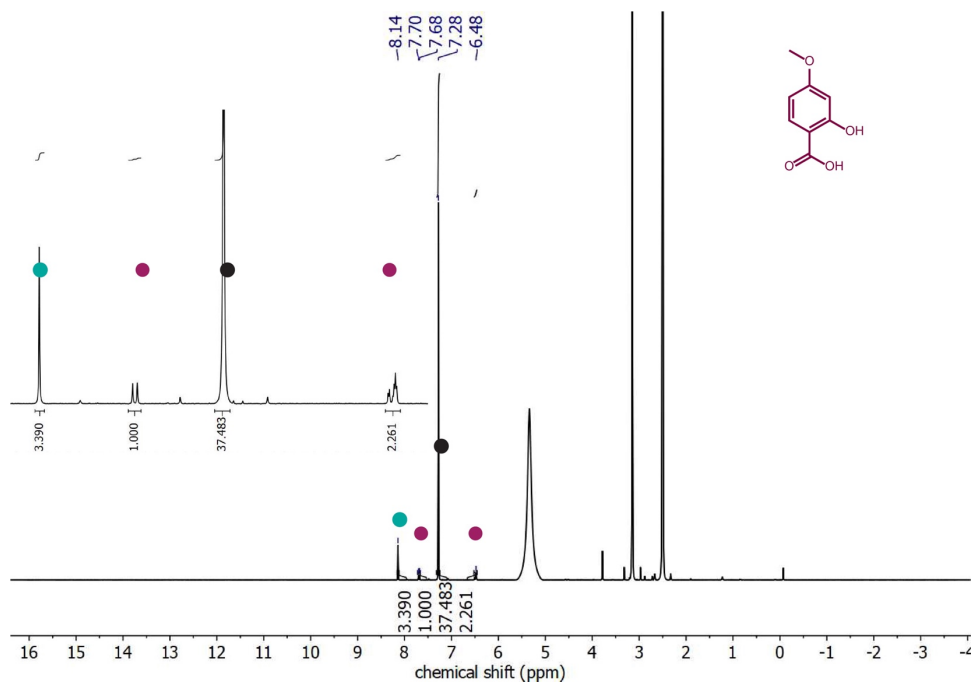


Figure S55. ¹H-NMR (400 MHz, DMSO-d₆) of Co₂(dobdc) nanorods synthesized with 2 equivalents of 4-methoxysalicylic acid. Light purple dots correspond to 4-methoxysalicylic acid protons. The black dot corresponds to H₂dobdc protons, and the teal dot corresponds to formate protons.

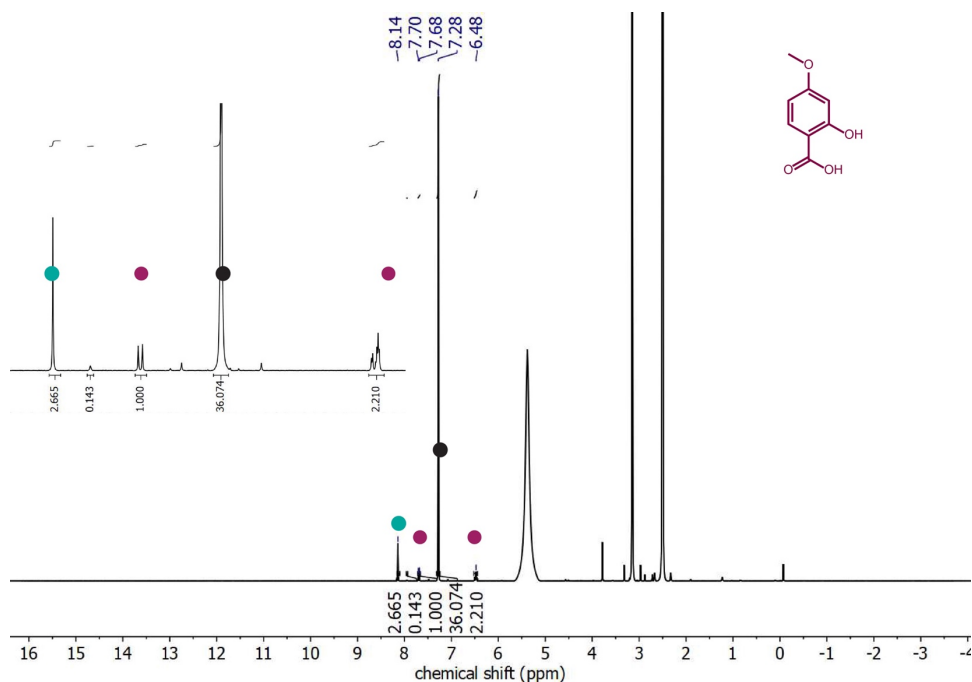


Figure S56. ¹H-NMR (400 MHz, DMSO-d₆) of Co₂(dobdc) nanorods synthesized with 3 equivalents of 4-methoxysalicylic acid. Light purple dots correspond to 4-methoxysalicylic acid protons. The black dot corresponds to H₂dobdc protons, and the teal dot corresponds to formate protons.

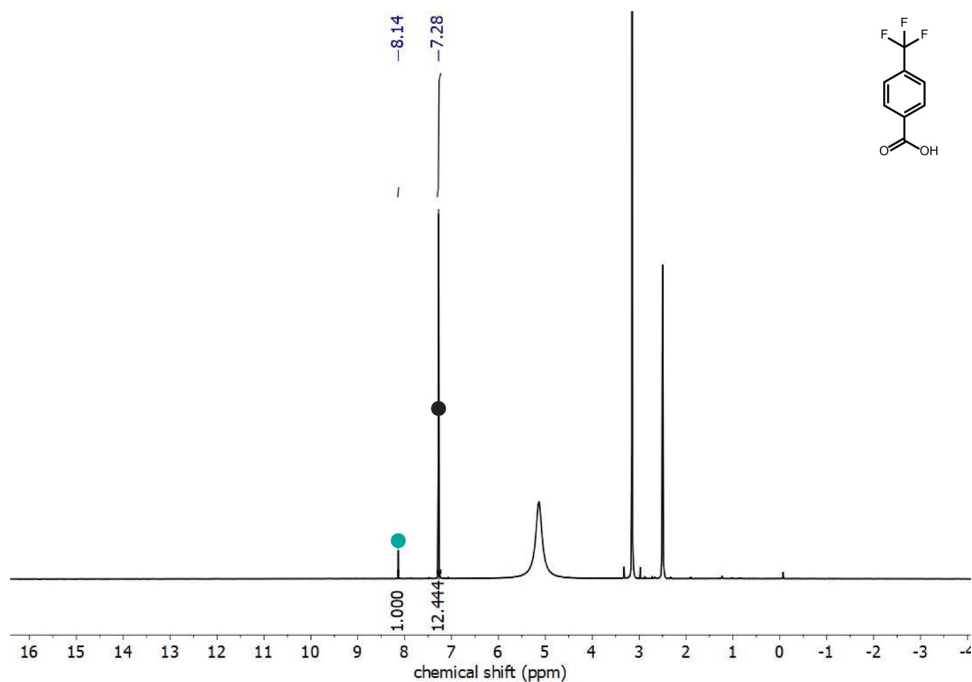


Figure S57. ¹H-NMR (400 MHz, DMSO-d₆) of Co₂(dobdc) synthesized with 1 equivalent of 4-trifluoromethylbenzoic acid. The black dot corresponds to H₂dobdc protons, while the teal dot corresponds to formate protons.

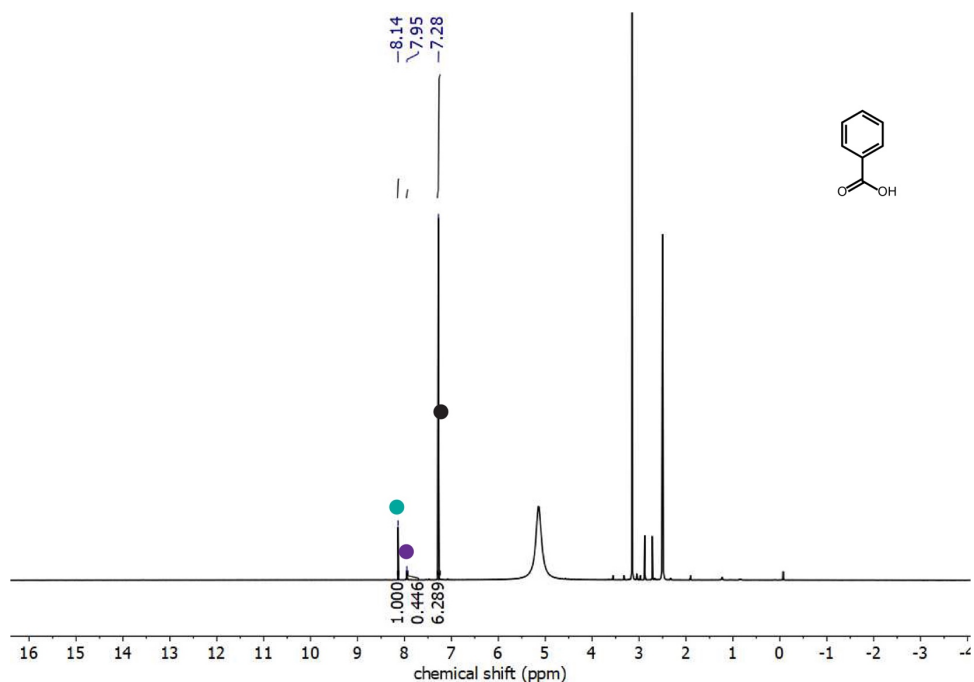


Figure S58. ¹H-NMR (400 MHz, DMSO-d₆) of Co₂(dobdc) synthesized with 1 equivalent of benzoic acid. The black dot corresponds to H₂dobdc protons, while the teal dot corresponds to formate protons. Dark purple dots correspond to DMF protons.

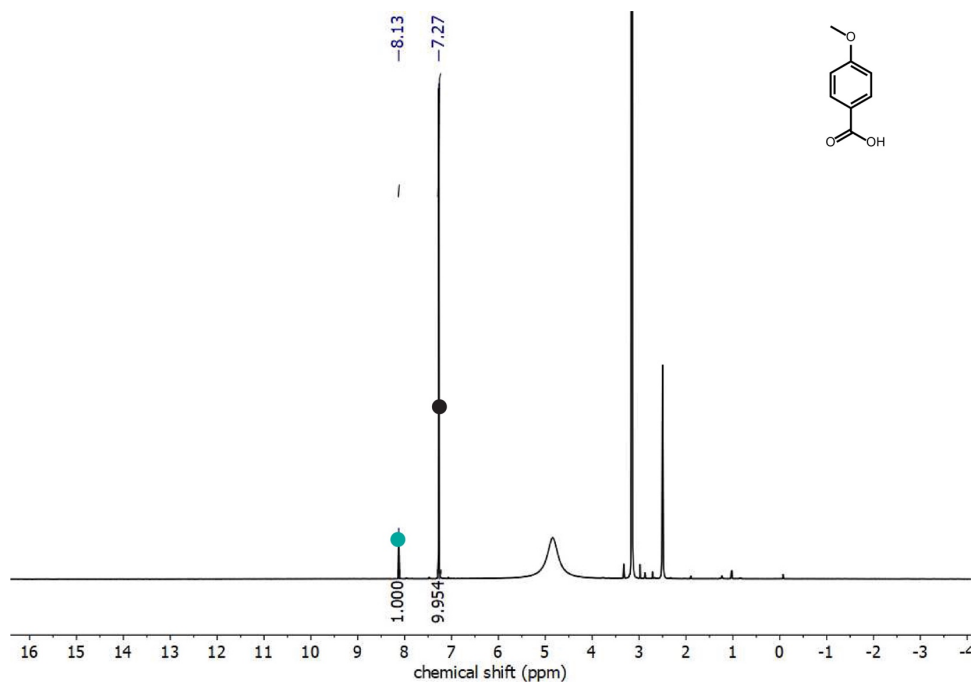


Figure S59. ¹H-NMR (400 MHz, DMSO-d₆) of Co₂(dobdc) synthesized with 1 equivalent of 4-methoxybenzoic acid. The black dot corresponds to H₂dobdc protons, while the teal dot corresponds to formate protons.

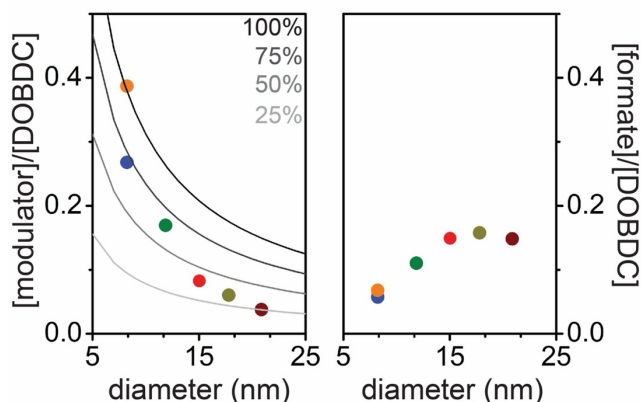


Figure S60. . Ligand ratios of $\text{Co}_2(\text{dobdc})$ nanorods synthesized with 1 equivalent of various salicylic acid modulators as measured by NMR. Expected ligand ratios for various surface coverage percentages are shown as solid lines.

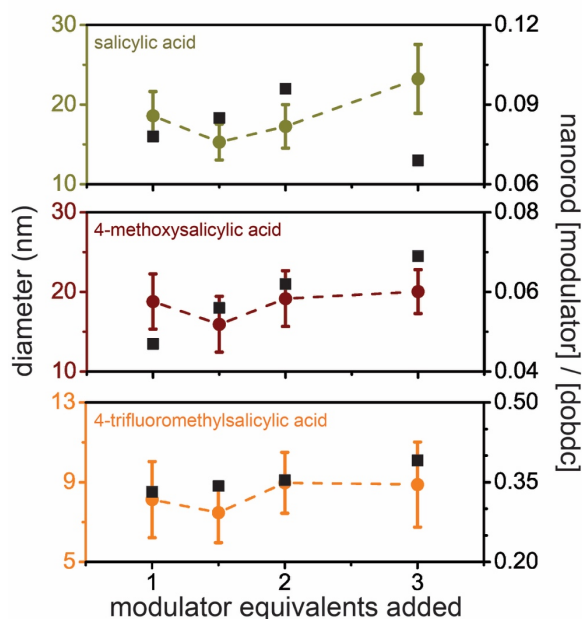


Figure S61. . Nanorod diameter distributions (circles) as measured by transmission electron microscopy are compared to modulator-to-bridging ligand ratios (squares) as measured by NMR of digested samples for $\text{Co}_2(\text{dobdc})$ nanorods synthesized with varying equivalents (relative to metal concentration) of salicylic acid, 4-methoxysalicylic acid, and 4-trifluoromethylsalicylic acid. Dashed lines highlight trends in nanorod diameter.

Table S1. Relative quantities of capping agents in MOFs synthesized with salicylic acid before and after exchange with 4-trifluoromethylsalicylic acid.

synthesis	# modulator	# formate	# H_2DOBDC	(mod+formate)/DOBDC
Salicylic acid only	1	2.30	13.8	0.24
Surface exchanged	1	0.33	5.18	0.25

External Surface Coverage Model

To estimate the extent of modulator surface coverage, Co₂(dobdc) nanorods were modeled as hexagonal prisms. By assuming that the modulator exclusively coats the nanorod external surface and that there are no defects in the nanorod, the total number of modulators can be modeled as a function of the nanocrystal external surface area via the following equation:

$$M_{NC} = \left(\frac{M_{UC}}{SA_{UC}} \right) SA_{NC} \quad (1)$$

where M_{UC} and M_{NC} represent the maximum number of modulator ligands in the unit cell and in the nanocrystal, respectively. M_{UC} can be obtained by counting the number of bridging ligands extending from the structure's unit cell. SA_{UC} refers to the surface area of the unit cell, which can be derived from the unit cell dimensions, and SA_{NC} refers to the surface area of the nanocrystal, which can be calculated from lengths and diameters measured via transmission electron microscopy.

Similarly, the number of bridging ligands can be calculated as a function of the nanocrystal volume, under the assumption that the bridging ligands reside exclusively in the internal structure of the nanorod, via the following equation:

$$D_{NC} = \left(\frac{D_{UC}}{V_{UC}} \right) V_{NC} \quad (2)$$

where D_{UC} and D_{NC} represent the number of bridging ligands in the unit cell and the nanocrystal, respectively. V_{UC} represents to the volume of the unit cell, while V_{NC} represents the volume of the nanocrystals, which can be calculated from the average lengths and diameters determined via transmission electron microscopy.

For the Co₂(dobdc) unit cell, the following values were obtained:

$$\frac{M_{UC}}{SA_{UC}} = \frac{2.87}{\text{nm}^2} \quad (3)$$

$$\frac{D_{UC}}{V_{UC}} = \frac{4.12}{\text{nm}^3} \quad (4)$$

The ratio of modulator ligands to bridging ligands can then be expressed as:

$$\frac{M_{NC}}{D_{NC}} = \left(\frac{x}{100} \right) \frac{\left(\frac{2.87}{\text{nm}^2} \right) (6ah)}{\left(\frac{4.12}{\text{nm}^3} \right) \left(\frac{3\sqrt{3}}{2} a^2 h \right)} = \left(\frac{x}{100} \right) \frac{1.6}{a} \quad (5)$$

where x represents the fraction of external surface coverage, a is the hexagon edge length, and h is the nanocrystal height (or length). Using the relationship between a hexagon's side and diameter ($d=2a$), the equation above can ultimately be rewritten in terms of the nanocrystal's diameter (d):

$$\frac{M_{NC}}{D_{NC}} = \left(\frac{x}{100} \right) \frac{3.12}{d} \quad (6)$$

Hammett Plot

Standard Hammett plots are generated for reactions that utilize benzoic acid derivatives using the following equation:

$$\log\left(\frac{K}{K_0}\right) = \sigma\rho \quad (7)$$

where K represents the equilibrium constant for a reaction of interest, K_0 is the equilibrium constant of a reference reaction, and σ is the substituent constant for each benzoic acid derivative. The reaction constant, ρ , can be either greater than 1 or less than 1. If $\rho > 1$, the reactions of interest are said to be governed by the same principles that dictate acidity.

For our system, K represents the equilibrium constant for the modulator–metal coordination reaction:



Similarly, K_0 represents the equilibrium constant for the bridging ligand–metal coordination reaction:



The relative equilibrium constants for these reactions can be represented as the ligand ratios:

$$\log\left(\frac{K}{K_0}\right) = \log\left(\frac{M_{NC}}{D_{NC}}\right) = \sigma\rho \quad (10)$$

Note that we used the σ values of analogous benzoic acid molecules as a proxy for those of the salicylic acid modulators.⁴ M_{NC} and D_{NC} were measured via NMR of digested samples.

Modulator pK_a Values

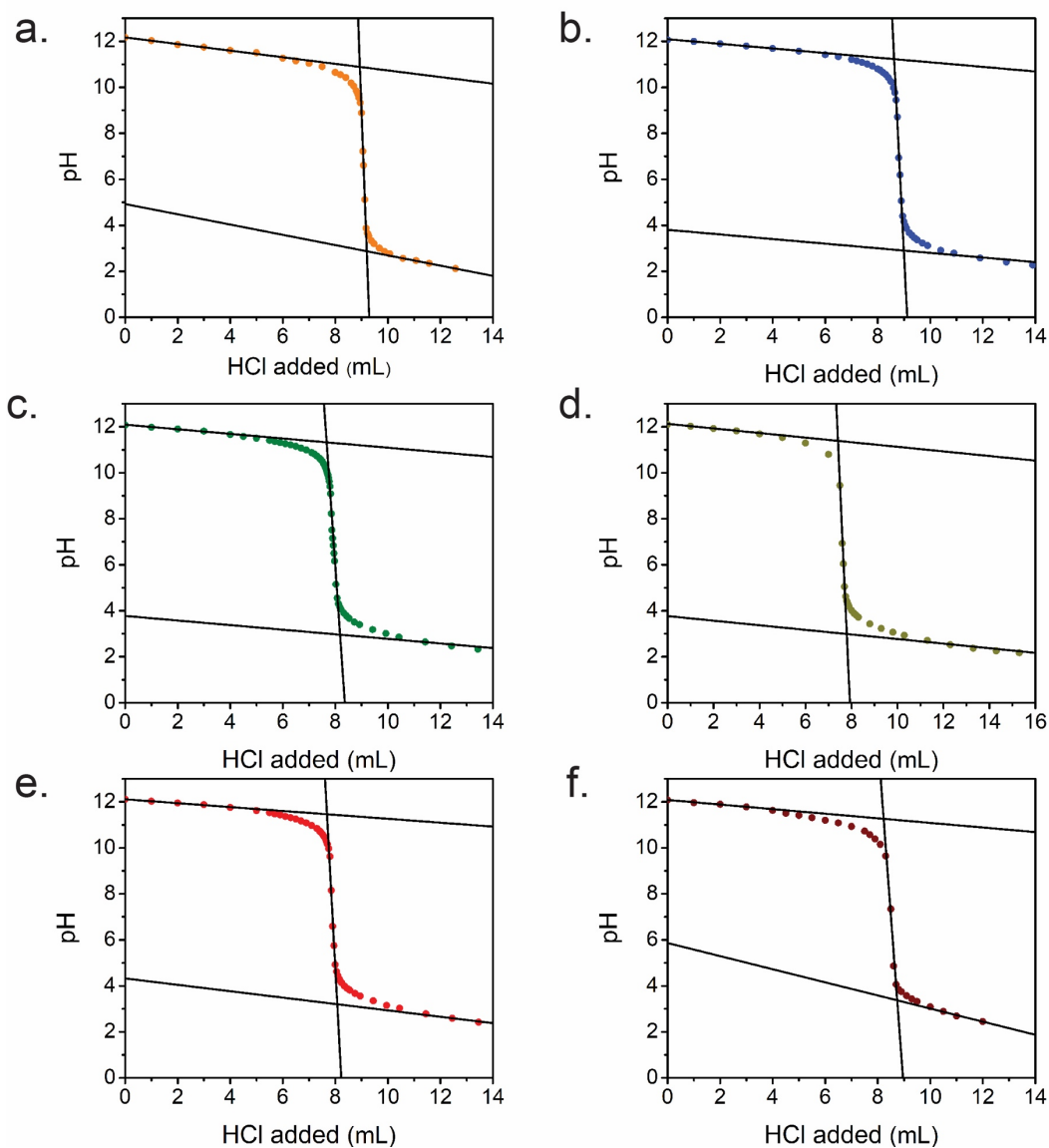


Figure S62. Aqueous pK_a titrations of (a) 4-trifluoromethylsalicylic acid (b) 4-bromosalicylic acid, (c) 4-fluorosalicylic acid, (d) salicylic acid, (e) 4-methylsalicylic acid, and (f) 4-methoxysalicylic acid. Lines indicate fits used to determine pK_a values of the carboxylic acid groups.

Table S2. Summary of the pK_a of the carboxylic acid functional group for all modulators used in this work.

Modulator	pK_a
4-methoxysalicylic acid	3.71
4-methylsalicylic acid	3.66
Salicylic acid	3.56
4-fluorosalicylic acid	3.54
4-bromosalicylic acid	3.50
4-trifluoromethylsalicylic acid	3.44

References

- (1) W. Yan, Z. Guo, H. Xu, Y. Lou, J. Chen, Q. Li, *Mater. Chem. Front.*, 2017, **1**, 1324-1330.
- (2) W. L. Queen, M. R. Hudson, E. D. Bloch, J. A. Mason, M. I. Gonzalez, J. S. Lee, D. Gygi, J. D. Howe, K. Lee, T. A. Darwish, M. James, V. K. Peterson, S. J. Teat, B. Smit, J. B. Neaton, J. R. Long, C. M. Brown, *Chem. Sci.*, 2014, **5**, 4569-4581.
- (3) K. S. Walton, R. Q. Snurr, *J. Am. Chem. Soc.*, 2007, **129**, 8552-8556.
- (4) L. P. Hammett, *J. Am. Chem. Soc.*, 1937, **59**, 96-103.